FE analyses of long-term creep deformations related to embankments and excavations

Master's Thesis in the Master's Programme Structural Engineering and Building Technology

Andreas Holmqvist

FE analyses of long-term creep deformations related to embankments and excavations

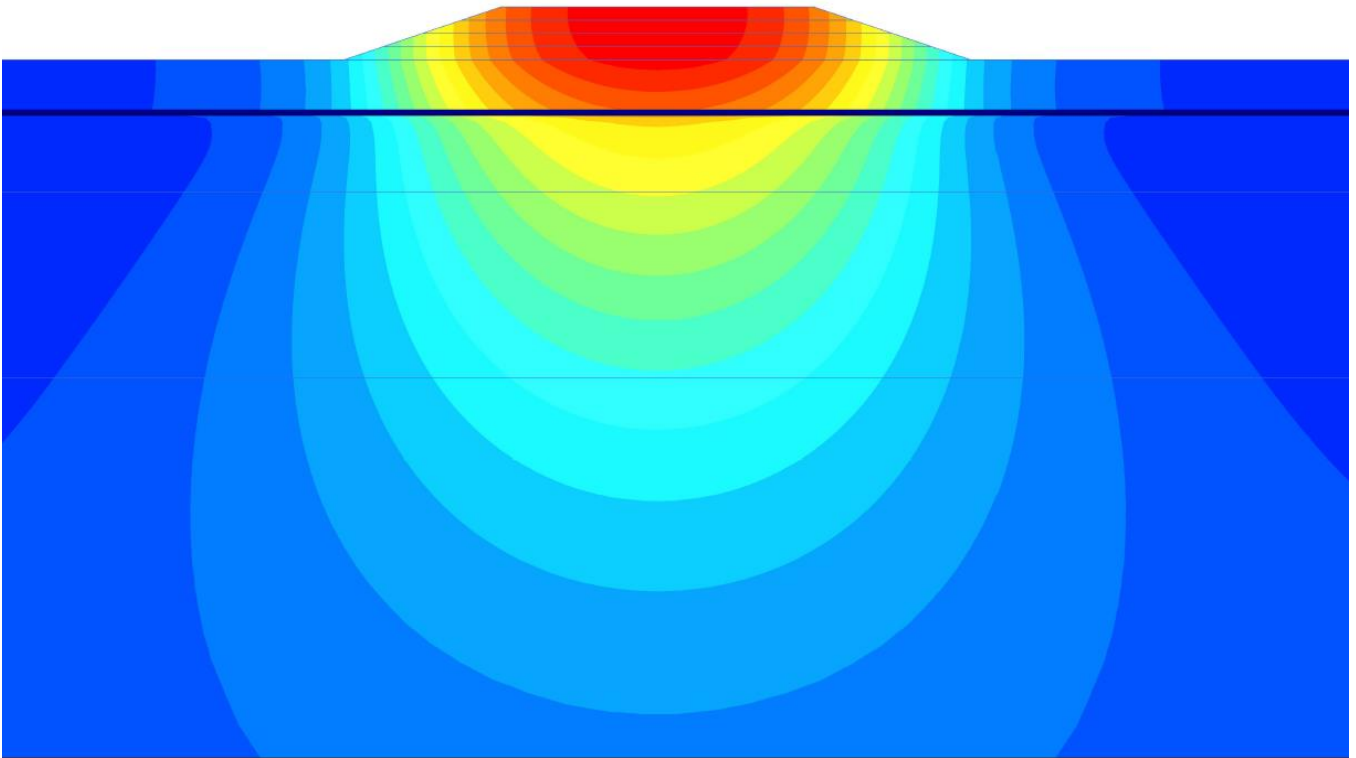*Master's Thesis in the Master's Programme Structural Engineering and Building Technology*

Andreas Holmqvist

FE analyses of long-term creep deformations related to embankments and excavations

Master's Thesis in the Master's Programme Structural Engineering and Building Technology

Andreas Holmqvist

Department of Civil and Environmental Engineering
Division of GeoEngineering
Geotechnical Engineering Research Group
Chalmers University of Technology
SE-412 96 Göteborg
Sweden
Telephone: + 46 (0)31-772 1000

Cover:
Plaxis 2D, contours showing the total displacement in regard of embankment problem

FE analyses of long-term creep deformations related to embankments and excavations

Master's thesis in the Master's Programme Structural Engineering and Building Technology

Andreas Holmqvist

Department of Civil and Environmental Engineering
Division of GeoEngineering
Geotechnical Engineering Research Group
Chalmers University of Technology

ABSTRACT

This MSc thesis uses the advantage of numerical modelling in order to predict soil behaviour. Nowadays, the more advanced numerical models in the field of geotechnics include creep to predict geotechnical problems in order to reduce uncertainty regarding long-term settlements. The model used for this thesis is the User Defined Soil Model (UDSM), creep-SLCAY1S model, in 2D Plaxis.

The first objective of this project was to study the soils long-term conditions in regard to embankment/excavation problems. Until now, no analysis in regard to unloading problems has been made with the creep-SCLAY1S model. The models aim is to include creep, destructuration and anisotropy by incorporating parameters that are associated to capture the soils behaviour. Parameters used for the models have been established by field measurements used in previous research projects. The lab tests were conducted on slightly over-consolidated silty clay/clayey silt, collected with the help of high quality samplers, mini block and piston (STII) from a test site in Utby, Gothenburg.
The second objective was to investigate different aspects of the models in form of sensitivity analysis, stress and shear strength determination as well as establish the impact of anisotropy and destrucutration by inactivating related parameters.

Conclusions in the report verify that the majority of the mini block and piston (STII) cases predict significant difference in vertical and horizontal displacement for both the embankment and the excavation problems whereas the piston (STII) case overpredict the outcome in relation to the mini block case. Long-term creep shows largest influence for the embankment problem where creep still develops after 100 years of consolidation. For the excavation problem, creep stops to develop after 50 years.

Key words: Creep-SCLAY1S, Embankment, Excavation, Creep, Plaxis 2D, Anisotropy, Triaxial test, OCR value, Modified Cam Clay, Modified compression index, Modified swelling index.

Finita element-analyser av krypsättningar med avseende på vägbankar och utgrävningar

Examensarbete inom masterprogrammet Structural Engineering and Building Technology

Andreas Holmqvist

Institutionen för bygg- och miljöteknik
Avdelningen för Geologi och Geoteknik
Forskargruppen för Geoteknik
Chalmers tekniska högskola

SAMMANFATTNING

Detta examensarbete använder fördelen av numerisk modellering för att förutsäga jordens beteende. Numera inkluderar de mer avancerade numeriska modellerna inom geoteknik kryp för att minska osäkerheten av långtids sättningar. Den modell som används för denna avhandling är creep-SLCAY1S modellen i 2D Plaxis.

Det främsta syftet med detta projekt var att studera jordens långsiktiga förutsättningar för vägbanks och utgrävnings problem. Hittills har ingen analys utförts med hänsyn till utgrävnings problem med creep-SCLAY1S modellen. Modellens mål är att fånga kryp, bindningen mellan jordpartiklarna och anisotropi genom att integrera de parametrar som är associerade och därav fånga jordens beteende. De parametrar som användes för modellerna har fastställts genom fältmätningar som använts i tidigare forskningsprojekt. De laboratorietester som var utförda var på lätt konsoliderad finkornig lera/lerig silt vilket genomfördes med hjälp av högkvalitativa block och kolv jordprover från en testplats i Utby, Göteborg.
Det andra målet var att undersöka olika aspekter av modellerna i form av känslighetsanalys , spänning och skjuvhållfasthet samt att fastställa effekten av anisotropi och bindningen mellan jordpartiklarna genom att inaktivera relaterade parametrar.

Slutsatser i rapporten verifierar att majoriteten av block och kolv fallen förutsäger signifikant skillnad i vertikal och horisontell förskjutning för både vägbanks och utgrävnings problemen där kolv parameterna överskattar utfallet i förhållande till block parametrarna. Långsiktig kryp visar störst inflytande vid vägbanks problem där kryp deformationerna fortskrider efter 100 år av konsolidering. För de utgrävnings problem som analyserades slutar kryp deformationerna efter 50 år.

Nyckelord: Creep-SCLAY1S, Vägbank, Utgrävning, Kryp, Plaxis 2D, Anisotropi, Triaxial test, OCR värde, Modified Cam Clay, Modifierad kompressionsindex, Modifierad svällningsindex.

Contents

Preface

This MSc thesis was carried out as a co-operation between the geotechnical engineering department at Norconsult and the division of geotechnical engineering at Chalmers University of Technology. It was conducted at Norconsult, Gothenburg, between January 18th and June 10th in 2016.

I would like to take this opportunity to thank my supervisor at Chalmers, Minna Karstunen, that provided frequent assistance through the whole MSc thesis.

I would also like to express my gratitude towards Bernhard Gervide Eckel and Rasmus Trygg at the geotechnical department at Norcosult for showing intersest in making this thesis possible and helped with the many problems I have encountered.

Gothenburg, June 2016

Andreas Holmqvist

Notations

Roman upper case letters

C_α	Secondary compression index
E	Young´s modulus
E_{oed}^{ref}	Reference oedometric modulus
G	Shear modulus
H	Drainage length
K	Bulk modulus
K_0	Coefficient of earth pressure in-situ
K_0^{nc}	Coefficient of earth pressure for normally consolidated soil
M	Slope of the critical state line
$M_{compression}$	Slope of critical state line for triaxial compression
$M_{extension}$	Slope of critical state line for triaxial extension
$M_{plane\ strain}$	Slope of critical state line in plane strain
R	Time resistance
T_v	Time factor

Roman lower case letters

a	Control rate of destructuration
b	Control rate of destructuration
c_v	Coefficient of consolidation
e	Void ration
e_0	Initial void ratio
f	Function of the yield surface
g	Plastic potential
k_x	Horizontal permeability
k_y	Vertical permeability
p'	Mean effective stress
p'_0	Mean effective pre-consolidation stress
p'_{eq}	Equivalent mean stress
p'_m	Mean effective pre-consolidation stress
p'_{mi}	Intrinsic mean effective pre-consolidation stress
p'_p	Hardening law for volumetric compression
q	Deviatoric stress
r_s	Creep resistance number
t	Time
v_k	Specific volume in unloading state
x	Amount of bonding in the soil

Greek lower case letters

α	Rotational hardening parameter
α_0	Initial inclination of the yield surface
$\alpha_{K_0^{nc}}$	Rotational hardening parameter for normally consolidated soil
α_s	Secondary consolidation index
β	Creep ratio
γ_{sat}	Unit weight saturated soil

γ_{unsat} Unit weight unsaturated soil
ε_p^e Increment of elastic volumetric strain
ε_q^e Increment of elastic deviatoric strain
ε_p^p Increment of plastic volumetric strain
ε_q^p Increment of plastic deviatoric strain
$\dot{\varepsilon}_p^e$ Elastic volumetric creep strain
$\dot{\varepsilon}_q^e$ Elastic deviatoric creep strain
$\dot{\varepsilon}_p^c$ Volumetric creep strain
$\dot{\varepsilon}_q^c$ Deviatoric creep strain
η Stress ratio
$\eta_{K_0^{NC}}$ Stress ratio in normally consolidated state
κ Swelling index
κ^* Modified swelling index
λ Compression index
λ_i Slope of intrinsic compression line
λ^* Modified compression index
μ Creep index
μ^* Modified creep index
v Poisson´s ratio
v_{ur} Poisson´s ratio for unloading
ξ Rate of destructuration
ξ_d Rate of destructuration by deviatoric strain
σ_1 Major principal stress
σ_2 Intermediate principal stress
σ_3 Minor principal stress
σ_d Vertical deviatoric stress
σ_p' Vertical pre-consolidation stress
σ_{v0}' Initial effective stress
τ Reference time
φ Friction angle
φ' Effective friction angle
Ψ Dilatancy angle
θ Lode angle
χ_0 Initial amount of bonding
$\dot{\Lambda}$ Creep rate
ω Controls the absolute rate of rotation
ω_d Controls the rate of rotation by deviatoric strain

Abbreviations

CSL Critical State Line
CSS Current State Surface
IL Incremental Loading
MCC Modified Cam Clay
NC Normal Consolidation
NCS Normal Consolidation Surface
OCR Over-Consolidation Ratio

1 Introduction

The introduction chapter in this MSc thesis is to provide an informative background to the problem and define the purpose and objectives along with a description of the methodology and limitations.

1.1 Background

Long-term settlements are an important aspect in the field of geotechnics, especially in areas with deep deposits of soft clay. It´s essential to accurately predict the settlement in various construction situations to prevent high maintenance costs as well as damage to structures. This MSc thesis aims to provide results in both the theoretical and practical field of geotechnics.

In this MSc thesis the effects of consolidation and long-term creep will be analysed using the creep-SCLAY1S model in 2D PLAXIS as a User-Defined Soil Model (UDSM). This model is an extension of the creep-S-CLAY1 model to account for the effect of destructuration. No or limited data has been collected with this new model with aspect of numerical modelling by embankments and excavations problems. The model uses creep behaviour of anisotropic clay to overcome the issue regarding volumetric creep strain. Other models such as the Soft soil creep (SSC) model and the anisotropic creep model (ACM) have a tendency to overestimate the outcome of the result due to this creep strain (Karstunen et al. 2015).

The MSc thesis project is carried out as a co-operation between Norconsult and the division of geotechnical engineering at Chalmers.

1.2 Purpose & objectives of the study

The aim of this MSc thesis is to investigate creep behaviour of anisotropic clay using the creep-SCLAY1S model in 2D PLAXIS. This is performed with different geometries and sets of parameters for embankment and excavation problems to establish how the creep behaves in such cases.

The objectives of the thesis include:

- To investigate long-term behaviour of anisotropic clay for different embankment and excavation problems.

- To perform sensitivity analyses on essential parameters.

- To test different geometries and set of parameters in the model and use parameters from both standard piston- (STII) and mini-block soil samples.

- To make conclusions and discuss the credibility of the results.

1.3   Method

The methodology used in this MSc thesis has been to initially undertake literary studies in the field of geotechnics such as technical reports, previous master thesis and lecture notes. Geotechnical data was analysed and included in the numerical modelling. Among sources of information are *Geotechnical Modelling (2004)* and *Soil Behaviour and Critical State Soil Mechanics (1990),* by *David Muir Wood.* In addition, a technical draft report written by *Mats Karlsson, Anders Bergström* and *Jelke Dijkstra* published in 2015, where the majority of the set of parameters used in this MSc thesis where taken from. The parameters from their report where evaluated from various lab tests.

The approach after the literary study was accomplished where to model in 2D Plaxis. Different models for each embankment and excavation problem where performed with varying geometries and sets of parameters. Along with this process, the simulated results was evaluated. Last step where make a conclusion and discuss the credibility of the result together with some recommendations for further research.

1.4   Limitations

Limitations where set in this MSc thesis in order to carry out the problem within the proposed time limit. The following limitations was made:

- The attempt of different geometries is limited to three geometries, for both the embankment and excavation problems.

- Theory involving numerical models that are used other than the creep-SCLAY1S model is only to be described briefly.

- Problems other than embankment and excavation problems are not to be considered in this MSc thesis.

2 Background theory

In this chapter the consolidation process together with various creep parameters and lab tests is introduced. The soil behaviour that occur in connection with the consolidation process is rather complex and in order to understand the featured numerical models some general knowledge about consolidation and creep is described.

2.1 Primary- & secondary consolidation

Primary consolidation occurs when the effective stress increases in conjunction with a decrease in excess pore pressure. The soil behaviour after the primary consolidation has different terminologies such as secondary consolidation, secondary compression, time resistance and creep. Secondary consolidation is when all excess pore pressure has dissipated and a decrease in volume occurs under constant effective stress, see figure 2.1. However, it's important to acknowledge that creep strains are considered to be involved in both the primary- and secondary consolidation process (Peter Claesson, 2003).

The theory of consolidation was developed by Terzaghi in 1936 where he proposed a model to determine the degree of consolidation by performing oedometer tests. The theory of consolidation can be expressed as:

$$T_v = \frac{c_v}{H^2} t \tag{2.1}$$

Where c_v is the coefficient of consolidation, t is the time and H is the drainage length that is dependent on whether the sample is drained on one or both sides of the oedometer test.

In 1957 Šuklje assumed that creep strains occur during the whole consolidation process. The consolidation could be defined as a relationship between strain rate $\dot{\varepsilon}$, effective stress $\sigma^{'}$ and void ratio e. The strains are assumed to be time dependent and linked to the permeability, layer thickness and drainage conditions (Peter Claesson, 2003).
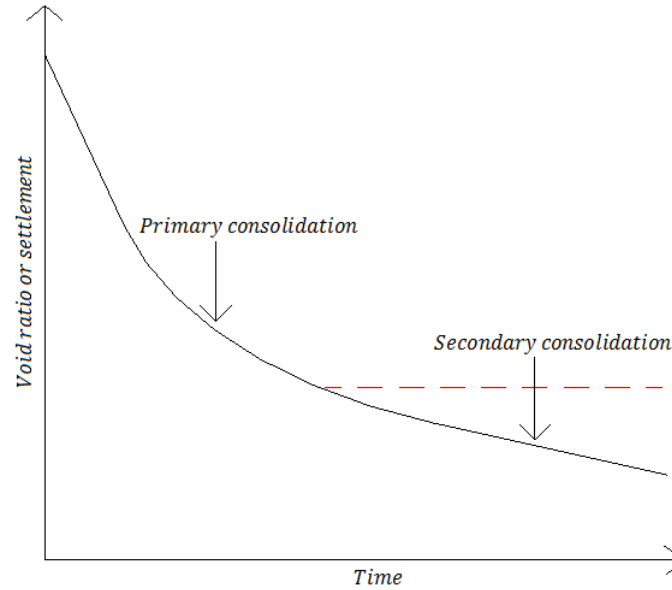
Figure 2.1: Phases of the primary- and secondary consolidation process

2.2   Over-Consolidation Ratio (OCR) & K₀

The stresses in the soil are highly influenced by its history were e.g. unloading and creep has occurred due to erosion (Mats Olsson, 2013). In order to determine the over-consolidation ratio (OCR) the degree of pre-consolidation stress σ_p' needs to be established. This can be done by performing one-dimensional oedometer tests or constant rate of strain (CRS) tests. OCR can be defined as the highest stress the soil has experienced divided by the current stress level.

$$OCR = \frac{\sigma_p'}{\sigma_{v0}'} \tag{2.2}$$

If $OCR = 1$ the soil is considered to be normally consolidated and for $OCR > 1$ over-consolidated.

In 1948 Jaky defined the coefficient of earth pressure at rest for normally consolidated soil, K_0^{NC}, by formulating an equation based on the effective critical friction angle ϕ' measured from triaxial tests.

$$K_0^{nc} = 1 - sin\phi' \tag{2.3}$$

However, in cases where the soil exhibit over-consolidation a modified equation was developed by Schmidt (1966).

$$K_0 = K_0^{nc} OCR^{1.2\sin(\phi')} \tag{2.4}$$

2.3 Oedometer test & general creep parameters

Three stiffness parameters are commonly used in commercial Plaxis creep models. These are the modified compression index λ^* and modified swelling index κ^* determined from the pre-consolidation phase. The modified creep index μ^* which is dependent of time rather than volumetric strain can be defined from the largest applied load performed in an incremental loading (IL) oedometer test. These stiffness and creep parameters can all be defined by performing one-dimensional oedometer tests, see figure 2.2. The difference between the modified parameters and the normally considered compression- and swelling index λ and κ is that the latter is defined by void ratio e instead of volumetric strains ε_p (Ronald B.J. Brinkgreve, 1999).
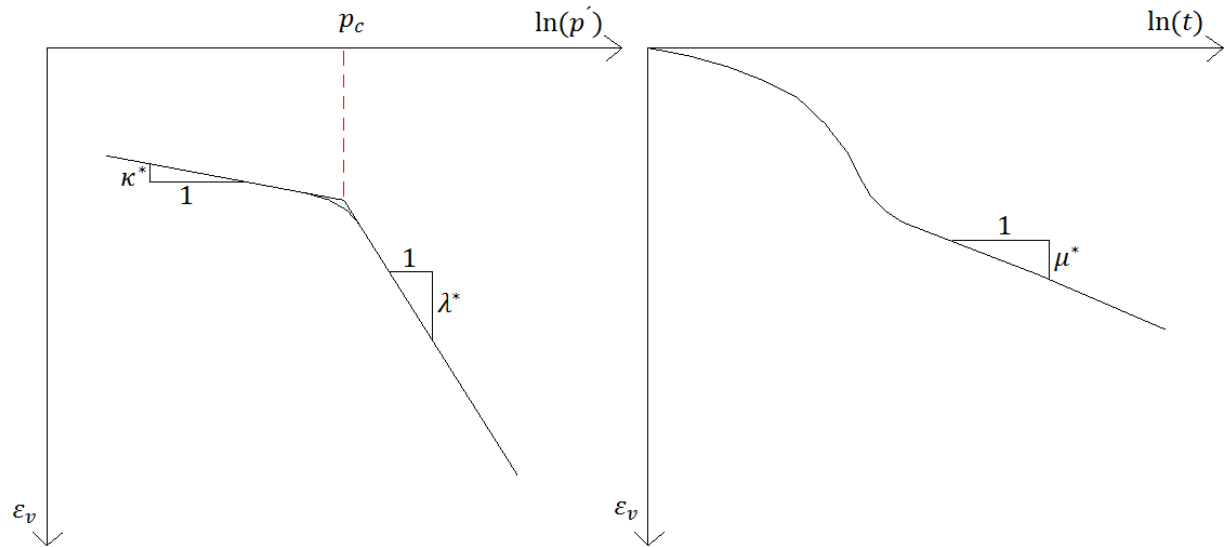

Figure 2.2: Showing the modified stiffness creep parameters in One-dimensional odeometer test

To convert from void ratio e to volumetric strain ε_p the following equations can be used.

$$\lambda^* = \frac{\lambda}{1+e} \tag{2.5}$$

$$\kappa^* = \frac{\kappa}{1+e} \tag{2.6}$$

$$\mu^* = \frac{1}{r_s} = \frac{C_\alpha}{ln10(1+e_0)} \tag{2.7}$$

These stiffness parameters are to be used in the creep-SCLAY1S model which is introduced in a later chapter in this MSc thesis.

To describe the creep behaviour in a soil the creep parameter C_α is defined as secondary compression index and is a function of void ratio e and time t. It can also be described as coefficient of secondary consolidation index α_s which is a function of creep strain ε_{cr} rather than void ratio e.

$$C_\alpha = \frac{\Delta e}{\Delta \log(t)}$$
(2.8)

$$\alpha_s = \frac{\Delta \varepsilon_{cr}}{\Delta \log(t)}$$
(2.9)

These parameters can be evaluated from performing incremental loading (IL) oedometer tests by assuming a log-scaled time interval. This usually is done in 24 hours interval where a load is successively applied. The secondary consolidation index is usually derived from the largest applied load performed in the oedometer test.

In 1969 Janbu introduced time resistance R to the field of geotechnics as an additional parameter to describe the creep behaviour of the soil. This can be defined as $Resistance = Cause/Effect$ and can be formulated with following equation (Grimstad et al, 2010):

$$R = \frac{dt}{d\varepsilon}$$
(2.10)

It has been proven by observations from one-dimensional compression tests that a linear relationship can be observed between time resistance R and time t. This relation is defined as the creep resistance number r_s which shows that the creep rate will decrease linearly with time (Mohammad Ali Haji Ashrafi, 2014).

$$r_s = \frac{dR}{dt}$$
(2.11)

2.4   Triaxial compression & extension test

The procedures of triaxial compression and extension tests can either be performed by increasing the axial stress $\sigma_1 = \sigma_a$ while the radial stresses $\sigma_2 = \sigma_3 = \sigma_r$ stays constant or by decreasing the radial stress while the axial stress stays constant, or a combination of both. By doing this it´s possible to deform and fail a test specimen (soil) based on its shear strength. The axial and radial stress can be defined as major and minor principal stress where the applied vertical deviator stress σ_d is the difference between σ_1 and σ_3, see figure 2.3. Main purpose of performing triaxial tests is to measure the undrained shear strength of the soil, it can also be used to measure the friction angle in drained conditions (R. H. G. Parry, 2005).
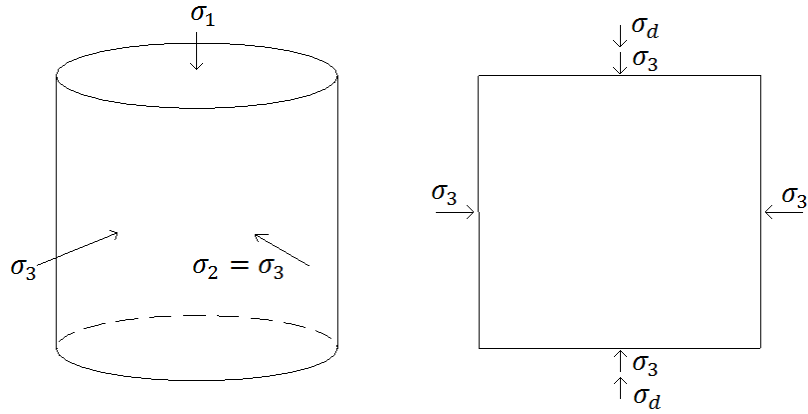
Figure 2.3: Principal stresses both during Axi-symmetric (left) and plain-strain (right) conditions

In order to fully perform the tests the initial applied stresses needs to be estimated as well as whether drained or undrained conditions or a combination of both during shear are of interest. The result is then plotted and is dependent of the soils fabric, drainage condition, stress history and applied stress (R. H. G. Parry, 2005). In these plots the relationship between deviator stress q and principal stress $p^{'}$ can be described as follows for axi-symmetric conditions.

$$q = \sigma_1 - \sigma_3 \tag{2.12}$$

$$p^{'} = \frac{1}{3}(\sigma_1 + 2\sigma_3) \tag{2.13}$$

Where the ratio between radial and axial stress during one-dimensional consolidation is given by

$$K_0 = \frac{\sigma_3^{'}}{\sigma_1^{'}} \tag{2.14}$$

This makes it possible to subject the test to either isotropic or anisotropic stress condition where the ratio between radial and axial stress is predetermined (R. H. G. Parry, 2004). The stress ratio is dependent on the type of soil and over-consolidation ratio (OCR).

2.5 Mini block & piston (ST II) sampler quality

The model parameters used in this MSc thesis are based on mini block and piston (STII) sampler. These parameters are stated in the technical draft report by *Mats Karlsson, Anders Bergström* and *Jelke Dijkstra* in 2015.

The Swedish piston (STII) sampler has a diameter of 50 mm which is pressed with SPT, CPT or other hollow rods down to a preferred depth at an even and low speed. It is designed to take undisturbed soil samples in clay, silt and fine sand. Only the middle part of the piston sampling are used to determine the quality assessments since the top and bottom part of the tube is considered to have been influenced by the sampling process.

The NTNU mini block sampler is a Norwegian invention developed at the Norwegian University of Science. The size of the mini block used for Mats Karlsson et al. 2015 technical report is approximately 300 mm high with a diameter of 165 mm. It's preferably to be used in clays and not in coarser soils. Compared with the Swedish piston (STII) sampler, the mini block sampler is more time consuming and expensive to use.

The laboratory tests are preferably performed close to the sampling date since temperature and humid conditions can provoke disturbance in the soil. It is also important to protect the sample from vibrations during transportation. A mini block sampler is in general expected to provide a higher level of quality by maintaining the soil in its original state whereas the piston (STII) has an increased risk to disturb the sample. In order to determine the quality of the mini block and piston (STII) sampler used in Mats Karlsson et al. 2015 technical report, a disturbance factor was established by looking at the in-situ void ratio e_0 contra Δe which represents the change in void ratio during re-consolidation. The sample disturbance factor is expressed as follows:

$$sdf = \frac{\Delta e}{e_0} \tag{2.15}$$

3 Constitutive models

In this chapter different models is introduced in order to get a deeper understanding of the more advanced creep-SCLAY1S model that is studied in this MSc thesis. This has been done through studies of previous developed models. The models are Modified Cam Clay (MCC), S-CLAY1, S-CLAY1S and creep-SCLAY1.

3.1 Modified Cam Clay (MCC)

The original Cam clay model was introduced by Roscoe and Schofield (1963). This model was then improved and named the modified Cam clay model. It is described as the first hardening plastic model which by now has become a basis for following soil models to come (Muir Wood, 1990). It has been particularly successful in analysing problems involving loading of soft clays and less so regarding loading problems on sand. The Cam clay models aim to capture the elastic and plastic deformations that occur within and on the yield surface, see figure 3.1. However, the model does not take into account all features of the soil (Muir Wood, 2004). For instance it is not suited for strain softening problems in numerical analyses for heavily over-consolidated soils, doesn't incorporate anisotropic soil behaviour and overpredicts the normal consolidated value of K_0^{NC} (Karstunen et al. 2008). Some of these problems are solved and improved in subsequently developed models.

The Cam clay model can be divided into four subcategories:

1. *Elastic/plastic properties*: The elastic behaviour as well as the plastic is assumed to be isotropic in the modified Cam clay model. It´s important to distinguish that an isotropic material can still have nonlinear soil behaviour (Muir Wood, 2004). Three stiffness parameters K(Bulk modulus), E(young´s modulus) and G(shear modulus) together with v(Poisson´s ratio) needs to be defined in order to describe the elastic soil behaviour. However, only two of these parameters are needed to establish the remaining two. The shear modulus G is set as a constant in the modified Cam clay model.

$$K = \frac{E}{3(1 - E2v)} \tag{3.1}$$

$$G = \frac{E}{2(1 + v)} \tag{3.2}$$

The relationship can be expressed as

$$G = K \frac{3(1 - 2v)}{2(1 + v)} \tag{3.3}$$

The specific volume v (not Poisson´s ratio) in the modified Cam clay model describes the ratio between total volume and the volume of the solid particles. Changes in v due

to loading can be expressed in the modified Cam clay model with the following exponential law:

$$v = v_\kappa - \kappa ln p'$$
(3.4)

Were κ is the swelling index and v_k is a reference value of the specific volume in the unload-reload state.

By assuming that shear modulus G and swelling index κ is constant the elastic deformations within the yield surface can be expressed as:

$$\delta\varepsilon_p^e = \frac{\delta p'}{K'} = \frac{\kappa}{v}\frac{\delta p'}{p'}$$
(3.5)

$$\delta\varepsilon_q^e = \frac{\delta q}{3G}$$
(3.6)

The elastic volumetric strains $\delta\varepsilon_p^e$ are dependent on increments in mean effective stress p' and bulk modulus K while the elastic deviatoric strains $\delta\varepsilon_q^e$ are dependent on deviatoric stress q and the soil's shear modulus G.
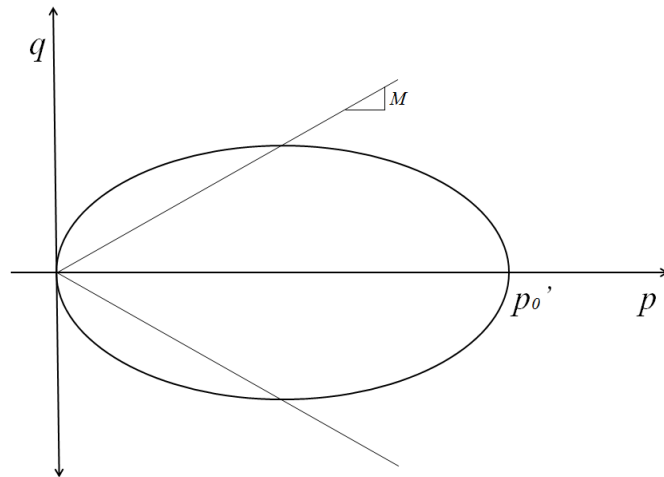

Figure 3.1: Shows how the yield surface is expressed in the modified Cam clay model

2. *Yield criterion*: In the Cam clay model the yield surface in a triaxial stress plane (p',q) is assumed to have an elliptical shape with equal size on both sides of the x-axis for computation simplicity. The collected data from compression or extension traixal tests determine the shape of the yield surface, i.e. where elastic soil behaviour turns to plastic hardening. The size of the ellipse is governed by the soils hardening parameter p_0', see figure 3.1. If the yield surface is defined as a function f the elastic behavior can be defined as $f < 0$ (within the yield surface). Yielding starts to occur if $f = 0$ (located on the yield surface) and cases where $f > 0$ (outside the yield surface) is not allowable. By also knowing the slope of the critical state line (CSL) of the ellipse, M can be established by performing triaxial tests in compression or extension, the following equations can be used to express M and the size of the yield surface (Muir Wood, 2004).

$$M_{compression} = \frac{6 sin\varphi'}{3 - sin\varphi'} \qquad (3.7)$$

$$M_{extension} = \frac{6 sin\varphi'}{3 + sin\varphi'} \qquad (3.8)$$

$$M_{plane\ strain} = \sqrt{3} sin\varphi' \qquad (3.9)$$

$$f(\sigma, p'_0) = \frac{q^2}{M^2} - p'(p'_0 - p') \qquad (3.10)$$

3. *Flow rule*: The flow rule defines the direction of the plastic strain increments whereas associated flow is assumed in Cam clay which means that the plastic increment vector $\delta\varepsilon^p$ is normal to the yield surface, see figure 3.2. A plastic potential function $g(\sigma)$ is incorporated to more accurately determine the flow rule instead of using the tangent to the yield surface to do so (Muir Wood, 1990). This entails that $g(\sigma) = f$ and can often be calculated in the same way as in equation (3.10). Plastic deformation depends on the changes in stress ratio $\eta = q/p'$ when yielding occurs. If however $\eta = M$ the yield surface is constant and no change in volume will occur, this is also referred as the critical state. If $\eta < M$ the yield surface will expand (strain hardening) and contract (strain softening) when $\eta > M$ (Muir Wood, 2004).
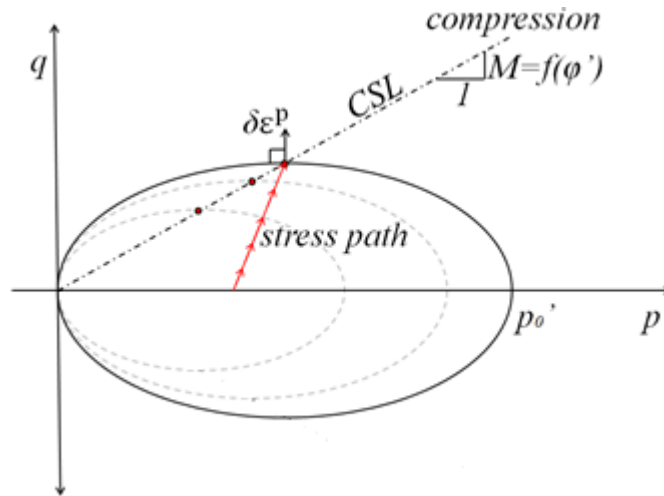

Figure 3.2: Shows the potential expansion of the yield surface in relation to the Critical State Line (CSL) in compression and extension

4. *Hardening rule*: If the flow rule describes the direction of the plastic strain increments, the hardening rule defines the magnitude. The magnitude of the yield surface expansion in Cam clay is only dependent of the relationship between the hardening parameter $\delta p'_0$ and plastic volumetric strains, $\partial p'_0 / \delta\varepsilon_p^p$ while as $\partial p'_0 / \delta\varepsilon_q^p = 0$ which provides the shape of the yield surface to remain the same, see figure 3.2. Through the variation of the hardening parameter p´₀ the size of the yield surface can be established and plastic volumetric strains can be calculated by

introducing an additional soil parameter λ which represent the plastic compressibility.

$$\delta \varepsilon_p^p = \frac{\lambda - \kappa}{v} \frac{\delta p'_0}{p'_0}$$
(3.11)

It has been shown in studies that the magnitude of the plastic strain is heavily dependent by the $\lambda - \kappa$ relationship (Muir Wood, 2004). The total volumetric strain can then be expressed by

$$\delta \varepsilon_p = \delta \varepsilon_p^e + \delta \varepsilon_p^p$$
(3.12)

3.2   S-CLAY1

In the modified Cam clay (MCC) model the soil is assumed to be isotropic with the same properties in all directions. Natural soils have, however deposited due to sedimentation and seasonal variations which cause soil properties in different directions (Muir Wood, 1990). This occurrence is called anisotropy and is accounted for in the S-CLAY1 model developed by Wheeler et al. (1997) and modified by Näätänen et al. (1999). If the horizontal stiffness differs from the vertical stiffness in the soil but every horizontal direction is identical, it's referred as cross-anisotropy (Muir Wood, 2004). By not including anisotropy, it may lead to inaccurate predictions including soil response under loading conditions. Elastic anisotropic soil behaviour is not incorporated in the S-CLAY1 model since it lead to increased complexity of the elastic soil behaviour and is fairly insignificant compared to the plastic soil behaviour in problems revolving loading of normally- or slightly over-consolidated clay (Karstunen et al. 2003).

The S-CLAY1 model uses similar formulations as the modified Cam clay model, but with the addition of a rotational hardening law accounting for anisotropy in the soil. Both plastic volumetric strain and plastic shear strain is assumed to contribute to the development of an inclined yield surface, see figure 3.3 (Karstunen et al. 2008).

Compared with the modified Cam clay (MCC) model, the S-CLAY1 model gives better predictions of the normal consolidated value K_0. S-CLAY1 is also more effective for practical use since it doesn't necessarily require additional soil testing. It´s mainly intended for normally consolidated or lightly over-consolidated soft clays. However, even if the S-CLAY1 model performs significantly better than the Cam clay model it has limitations where the effect of plastic straining due to gradual degradation of bonding called destructuration is not included (Karstunen et al. 2008). This is solved in the subsequent S-CLAY1S model.
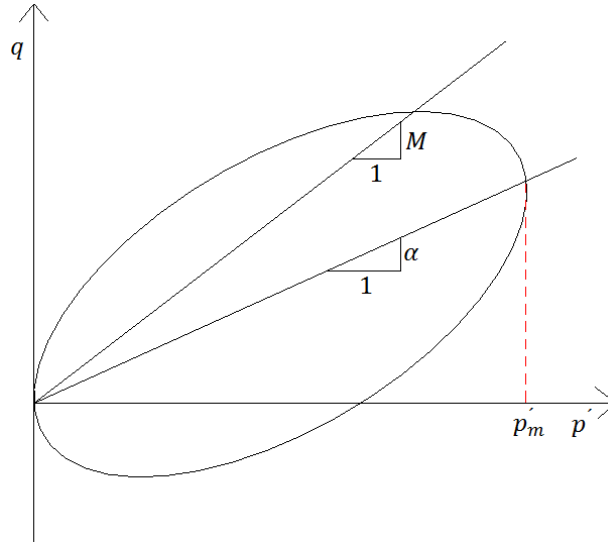
Figure 3.3: S-CLAY1 is represented with an inclined yield surface with the shape of an ellipsoid in a triaxial stress space

The equations based on the S-CLAY1 model is presented by triaxial test in form of $p^{'}$ (mean effective stress) and q (deviator stress) in the same way as for the modified Cam clay model. Different evidence has been proposed whether associated- or non-associated flow rule should be applied in combination with an inclined yield surface (Karstunen et al. 2003). For the S-CLAY1 model associated flow has however been assumed in interest of simplicity. The yield surface can be expressed by introducing a scalar parameter α which describes the rotation of the yield surface and $p^{'}_m$ which defines the mean effective pre-consolidation stress, see figure 3.3 (Karstunen et al. 2008).

$$f = (q - \alpha p^{'})^2 - (M^2 - \alpha^2)(p^{'}_m - p^{'})p^{'} = 0 \tag{3.13}$$

The value of M is calculated in the same way as for modified Cam clay indicating the slope of the critical state line (CSL). The same equations are also used to describe the isotropic elastic behaviour within the yield surface due to simplicity of the S-CLAY1 model. The hardening parameter $p^{'}_m$ is formulated by rephrasing equation (3.11) from the modified Cam clay model.

$$\delta p^{'}_m = \frac{v p^{'}_m}{\lambda - \kappa} \delta \varepsilon_p^p \tag{3.14}$$

By introducing a second hardening law associated with anisotropy, the rotation of the yield surface can be defined. This is done by measuring the rotation of the yield surface caused by increments of plastic volumetric strain and plastic shear strain (Karstunen et al. 2008). The yield surface rotation is defined by

$$\delta \alpha = \mu \left[\left(\frac{3\eta}{4} - \alpha \right) \langle \delta \varepsilon_p^p \rangle + \beta \left(\frac{\eta}{3} - \alpha \right) |\delta \varepsilon_q^p| \right] \tag{3.15}$$

Where β describes the relative effectiveness between plastic volumetric strains and plastic shear strains in rotating the yield surface. The value of μ is a constant which control the rate of rotation that is linked to the rotational hardening and $\eta = q/p^{'}$ is

the stress ratio. If however μ and α is set to zero the yield surface would resemble the one expressed in the modified Cam clay model.

3.3   S-CLAY1S

In addition to anisotropy generating the changes in the inclination of the yield surface, natural soils also exhibit initial bonding between the soil particles. The sensitivity of natural clay is linked to the amount of initial bonding. If the natural soil is deformed, the particle bonding is progressively destroyed by plastic straining and the soil reconstitutes (Yin and Karstunen, 2011). This is referred to as destructuration which is incorporated in the extended S-CLAY1S model developed by Koskinen et al (2002). The degradation of bonding is affected by a reduction in both plastic volumetric strains and plastic deviatoric strains (Karstunen et al. 2005). Furthermore the elastic soil behaviour is isotropic and associated flow rule is assumed.
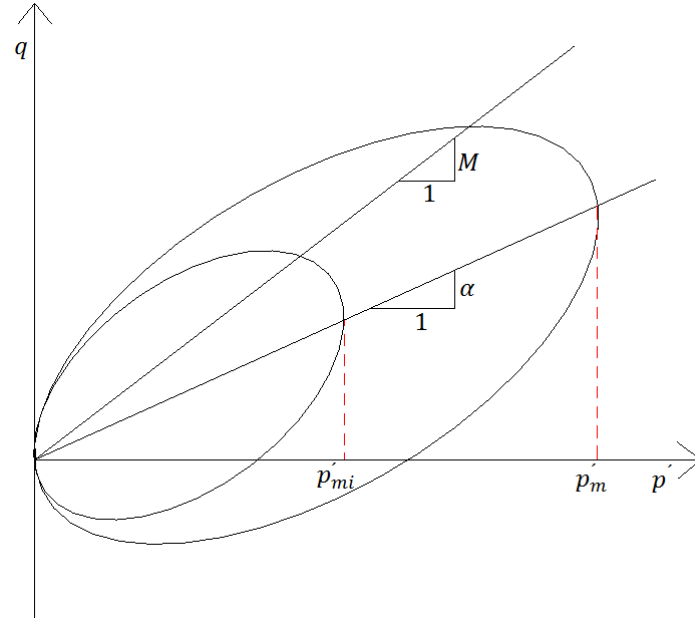

Figure 3.4: S-CLAY1S yield surfaces, the external yield surface represent the natural (undisturbed) yield surface and the intrinsic yield surface represent a reconstituted sample in a triaxial stress space

Due to the effect of destructuration, the yield criterion is now defined by one external and one intrinsic yield surface. The external yield surface is representing the natural (undisturbed) soil which account for bonding between the particles and the intrinsic representing the yield surface in the absence of bonds (Karstunen et al. 2005), see figure 3.4. The intrinsic yield surface can be expressed as

$$f = (q - \alpha p')^2 - (M^2 - \alpha^2)([1+x]p'_{mi} - p)p' = 0 \qquad (3.16)$$

$$\delta p'_{mi} = \frac{v p'_{mi}}{\lambda_i - \kappa} \delta \varepsilon_p^p \qquad (3.17)$$

Where x is the amount of bonding and p'_{mi} defines the intrinsic pre-consolidation pressure. If $x = 0$ however, no development of the bonds is assumed to have occurred

and the yield surface is equivalent to the one expressed in the S-CLAY1 model. The same two hardening laws explained in the Cam clay and S-SCLAY1 model is used in the S-CLAY1S model, describing the magnitude and rotation of the yield surface. But to incorporate destructuration of the soil a third hardening law is introduced.

$$dx = -ax\left(\left|d\varepsilon_p^p\right| + b\left|d\varepsilon_q^p\right|\right) \tag{3.18}$$

Where two additional soil constants a and b is used to control the rate of degradation (Karstunen et al. 2005).

The influence of destructuration is especially important for staged construction problems on sensitive natural soils were it may lead to a decrease in undrained shear strength in e.g. embankment problems. This often occurs in combination with an increase in remolded undrained shear strength.

It can be concluded that the S-CLAY1S model has the potential to capture many of the important soil aspects of soil behaviour. However the effect of creep is still not included in any of the models mentioned above which could be of great importance in a long-term perspective.

3.4   Creep-SCLAY1

Creep is essential to predict long-term settlement of different construction problems in natural soils. By extending S-CLAY1 model by wheeler et al. (1997) with the effect of creep, the creep-SCLAY1 model is introduced. Similar isotropic and anisotropic conditions and parameters are used as in the S-CLAY1 model, but with the addition of viscosity parameters which mean that the soil undergoes the effect of creep and rate dependency that is included in the model (Grimstad, 2010).

In combination with the elastic volumetric and deviatoric strain, elastic creep strain is incorporated and defined as follows:

$$\varepsilon_p = \dot{\varepsilon}_p^e + \dot{\varepsilon}_p^c \tag{3.19}$$

$$\varepsilon_q = \dot{\varepsilon}_q^e + \dot{\varepsilon}_q^c \tag{3.20}$$

The dot above the symbols indicate strain rate in respect to time and the subscripts e and c represents the elastic and creep components.
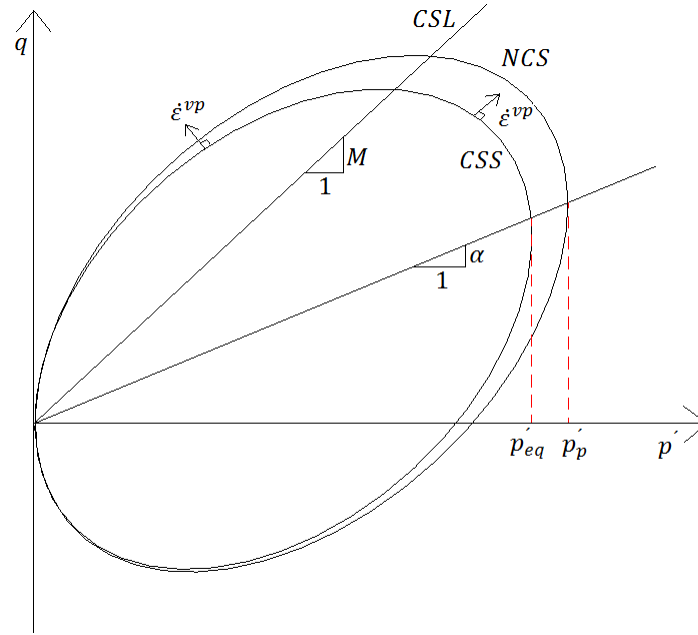
Figure 3.5: Creep-SCLAY1 yield surface, defining the Normal Consolidation Surface (NCS) and Current State Surface (CSS) in a triaxial stress space

In order to describe the size of the Normal Consolidation Surface (NCS) shown in figure 3.5, two stiffness parameters λ^* and κ^* is introduced together with volumetric creep strains ε_p^c to define the hardening law p_p'.

$$p_p' = p_{p0}' exp\left(\frac{\varepsilon_p^c}{\lambda^* - \kappa^*}\right) \tag{3.21}$$

Where λ^* is the modified compression index and κ^* is the modified swelling index which is presented in chapter 2.3. The inner ellipse represents the Current State Surface (CSS) that defines the current state of effective stress. The corresponding surface is called the equivalent mean stress p_{eq}' and is expressed as follows:

$$p_{eq}' = p' \frac{(q - \alpha p')^2}{(M^2(\theta) - \alpha^2)p'} \tag{3.22}$$

where

$$M(\theta) = M_c\left(\frac{2m^4}{1 + m^4 + (1 - m^4)sin3\theta_\alpha}\right)^{\frac{1}{4}} \tag{3.23}$$

Where the slope of the critical state line (CSL) M is dependent of the lode angle θ to provide a smooth surface in critical state. The value of m is defined as the ratio between slope of critical state line (CSL) in extension M_e and compression M_c measured from performing triaxial tests. In order to incorporate creep at constant rate, the visco-plasitc multiplier $\dot{\Lambda}$ is defined.

$$\Lambda = \frac{\mu^*}{\tau} \left(\frac{p'_{eq}}{p'_p}\right)^{\beta} \left(\frac{M^2(\theta) - \alpha_{K_0^{nc}}^2}{M^2(\theta) - \eta_{K_0^{nc}}^2}\right) \tag{3.24}$$

$$\beta = \frac{\lambda^* - \kappa^*}{\mu^*} \tag{3.25}$$

The creep ratio is defined as β which is defined by equation (3.25). τ in equation (3.24) is the reference time and is normally set to 24 hours since that's the step interval for a standard incremental loading (IL) oedometer test. $\alpha_{K_0^{nc}}$ and $\eta_{K_0^{nc}}$ is the rotation of the yield surface and stress ratio in normally consolidated state.

A modified rotational hardening law is used in the creep-SCLAY1 model to orientate the Normal Consolidation Surface (NCS) and incorporate the effect of anisotropy due to irrecoverable creep strains.

$$\delta\alpha = \omega \left[\left(\frac{3\eta}{4} - \alpha\right)\langle\delta\varepsilon_p^c\rangle + \omega_d \left(\frac{\eta}{3} - \alpha\right)|\delta\varepsilon_q^c|\right] \tag{3.26}$$

Where ω is a constant that controls the absolute rate of rotation of the yield surface which goal is to reach its target value of α. The value of ω_d is also a constant which controls the relative effectiveness of the volumetric creep strains ε_p^c and deviatoric creep strains ε_d^c.

By including the visco-plastic multiplier the creep strain rates can be expressed as.

$$\dot{\varepsilon}_p = \Lambda \frac{dp'_{eq}}{dp'} \tag{3.27}$$

$$\dot{\varepsilon}_q = \Lambda \frac{dp'_{eq}}{dq} \tag{3.28}$$

The subsequent creep-SCLAY1S model that is implemented as a User-Defined Soil Model (UDSM) in this MSc thesis is described in subsequent chapter 4.

4 Model

In this chapter the soil profile, finite element mesh, model stages and conditions are introduced together with the input parameters used in the creep-SCLAY1S model.

4.1 Finite element mesh

The model consists of 6-noded elements with refined mesh beneath the embankment/excavation where the largest settlements are expected to occur. This is done by the aid of two vertical lines drawn on both sides of the considered construction, see figure 4.1. The refined areas element size is set to 0.0625 meters and the coarser area is set to 1.0 meters. Total number of elements in the model is 15372 with 31105 nodes. Finer mesh generates an increased accuracy for the predicted outcome from the simulations. The quality of mesh can be defined by an aspect ratio in Plaxis that ranges from $0 - 1$, where a large value indicate high quality and vice versa. The majority of the refined mesh in the model has aspect ratio 1.0 with a few local elements with lower values. The same mesh distribution is used for both the embankment and excavation problems. The mesh distribution is illustrated in figure 4.1.
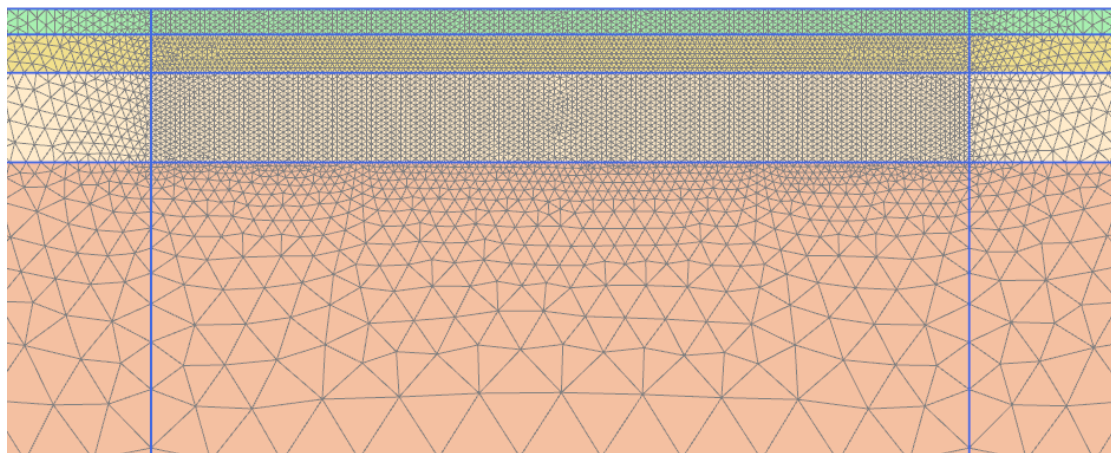

Figure 4.1: Profile of the mesh distribution

4.2 Embankment/excavation models

The model is analysed in plane strain conditions. Two different sets of parameters are used in the model, from both standard piston (STII) and mini-block samples collected from a test site in Utby close to the Gothenburg area. The user-defined creep-SCLAY1S model is used for the clay layers and Mohr-Coulomb for the embankment and dry crust layer.

A geometry profile of the model is presented in figure 4.2 that represent the soil layers, groundwater level as well as geometries of the embankment and construction. Total depth×width in the model is set to 40×200 meters with either an embankment or excavation in the centre of the model. A variation of embankment/excavation geometries is simulated and analysed in subsequent chapter 5.
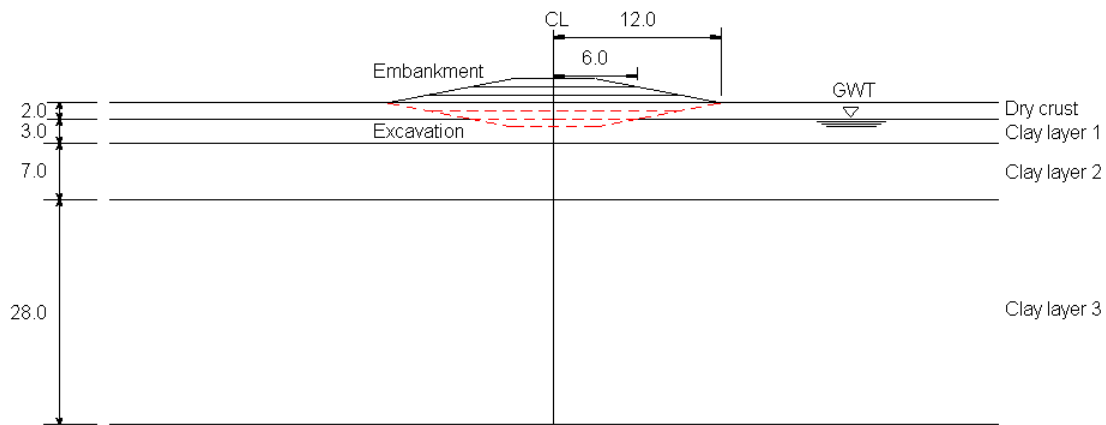
Figure 4.2: Geometry profile of the model showing soil layers and embankment/excavation construction

The models are divided into four soil layers with a groundwater table located 2 meters below the ground surface. The top layer consists of two meters dry crust and beneath is three layers slightly over-consolidated silty clay/clayey silt located. The OCR in the clay layers is however dependent on the sampler case being analysed. The hydraulic conductivity in the first two clay layers is set to $1 \cdot 10^{-9}$ m/s and in the third clay layer to $8 \cdot 10^{-10}$ m/s. Hydraulic boundary conditions are assumed to be open on all sides.

Consolidation and staged construction is chosen for the calculation phases. The construction time is assumed to be 4 days/meter constructed embankment or excavation. The recommended lifespan of a permanent geotechnical construction is at least 80 years according to TK-GEO, Trafikverket. The long-term settlements in this MSc thesis is analysed for 100 years. A summarization of the calculation process in the model is showed in table 4.1.

Table 4.1: Settings for the phases before, during and after the embankment/excavation construction in the model

Identification	Initial settings	Embankment/excavation construction	Creep settlement
Phase	Initial phase	Phases	Phases
Calculation type	K0 procedure	Consolidation	Consolidation
Loading type	Staged construction	Staged construction	Staged construction
Pore pressure calculation	Phreatic	Phreatic	Phreatic
Time	-	4 days/meter	100 years

4.3   Determination of Creep-SCLAY1S parameters

A total of 14 parameters are established in order to account for the isotropic, anisotropic, destructuration and viscous properties in the creep-SCLAY1S model. In addition 6 initial stress state parameters need to be defined to determine the stress state of the yield surface. In table 4.2 a compilation of the essential parameters in the creep-SLCAY1S model is illustrated. The estimated input values for the silty clay/clayey silt layers are found in appendix A.

Table 4.2: Creep-SCLAY1S parameters

Type	Parameters	Symbol
Isotropic Parameters	Modified swelling index	κ^*
	Modified intrinsic compression index	λ_i^*
	Poisson´s ratio	v
	Slope of Critical State Line (CSL) in compression	M_c
	Slope of Critical State Line (CSL) in extension	M_e
	Friction angle	$\varphi^{'}$
Anisotropic parameters	Initial inclination of yield surface	α_0
	Absolute effectiveness in rotational hardening	ω
	Relative effectiveness in rotational hardening	ω_d
Destructuration parameters	Initial bonding	χ_0
	Absolute rate of destructuration	ξ
	Relative rate of destructuration	ξ_d
Viscous parameters	Modified creep index	μ_i^*
	Reference time (days)	τ
Initial stress State parameters	Initial void ratio	e_0
	Unit weight for each layer [kN/m³]	$\gamma^{'}$
	Pre-consolidation pressure [kPa]	$p_c^{'}$
	Earth pressure at rest for NC soil	K_0^{NC}
	Over-consolidation ratio	OCR
	Pre-overburden pressure [kPa]	POP

The yield surface of the creep-SCLAY1S model is represented in figure 4.3. It defines the Normal Consolidation Surface (NCS), Current State Surface (CSS) and Intrinsic State Surface (ISS) in a triaxial stress space. In comparison with the previous creep-SCLAY1 model, it incorporates the effect of destructuration as is described in previous chapter 3.2.
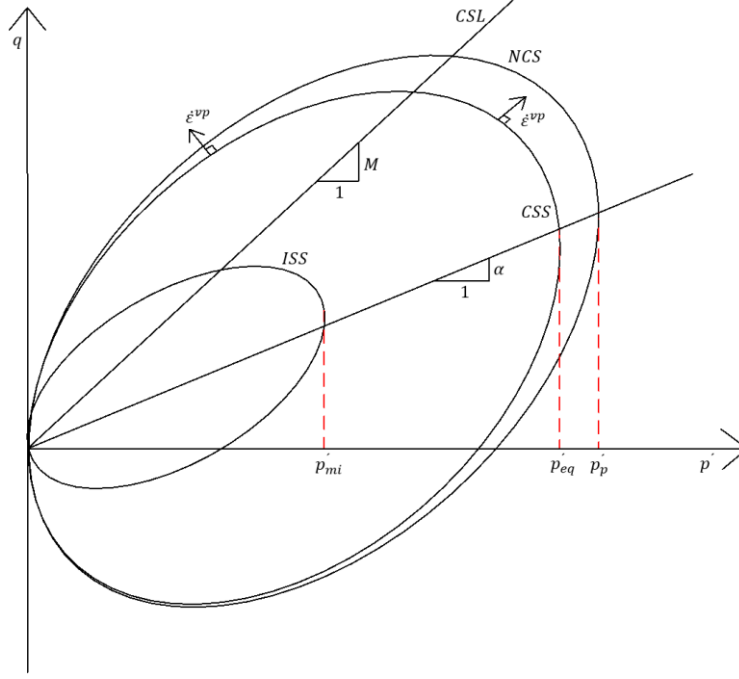
Figure 4.3: Creep-SCLAY1S yield surface, defining the Normal Consolidation Surface (NCS), Current State Surface (CSS) and Intrinsic State Surface (ISS) in a triaxial stress space

The visco-plastic multiplier defined in equation (4.1) uses in addition to equation (3.24) the amount of bonding χ and the intrinsic pre-consolidation pressure p'_{mi} defined in equation (3.17).

$$\dot{\Lambda} = \frac{\mu^*}{\tau} \left(\frac{p'_{eq}}{(1+\chi)p'_{mi}} \right)^{\beta} \left(\frac{M^2(\theta) - \alpha^2_{K_0^{nc}}}{M^2(\theta) - \eta^2_{K_0^{nc}}} \right) \tag{4.1}$$

The amount of initial bonding χ in the creep-SCLAY1S model depend on ξ and ξ_d. ξ controls the absolute rate of destructuration whereas ξ_d controls the relative rate of destructuration between volumetric and deviatoric strains.

$$d\chi = \xi\left([0-\chi]\left|d\varepsilon_v^p\right| + \xi_d[0-\chi]d\varepsilon_d^p\right) = -\xi\chi\left(\left|d\varepsilon_v^p\right| + \xi_d d\varepsilon_d^p\right) \tag{4.2}$$

A large proportion of the parameters used in this MSc thesis have already been established in the technical draft report published by Mats Karlsson, Anders Bergström and Jelke Dijkstra (2015). However, the anisotropic parameters used in the creep-SCLAY1S model are not stated. These parameters have a more theoretical approach and can be formulated based on the equations below.

By assuming one-dimensional consolidation the ratio between the plastic deviatoric strains and plastic volumetric strains is 2/3 (Mats Olsson 2013). It also requires that associated flow rule is considered. These assumptions make it possible to formulate the initial inclination α_{K0}.

$$\alpha_{K0} = \frac{\eta_{K0}^2 + 3\eta_{K0} - M_c^2}{3} \tag{4.3}$$

Where M_c is defined in equation (3.7) and the stress ratio η_{K0} is formulated as following:

$$\eta_{K0} = \frac{3(1 - K_0^{NC})}{(1 + 2K_0^{NC})} \tag{4.4}$$

By combining equation (4.1) with the assumption that $d\alpha = 0$ in equation (3.26) the scalar parameter ω_d can be expressed with the following equation:

$$\omega_d = \frac{3}{8} \frac{4M_c^2 - 4\eta_{K0}^2 - 3\eta_{K0}}{\eta_{K0}^2 - M_c^2 + 2\eta_{K0}} \tag{4.5}$$

Leoni et al. 2008 come to the conclusion that the absolute rate of rotation ω could be estimated based on the parameters α_{K0}, M, ω_d and λ^* with the criterion that ω is in-between the recommended interval (4.6).

$$\frac{10}{\lambda^*} \leq \omega \leq \frac{20}{\lambda^*} \tag{4.6}$$

$$\omega = \frac{1}{\lambda^*} ln \frac{10MM_c^2 - 2\alpha_0\omega_d}{M_c^2 - 2\alpha_0\omega_d} \tag{4.7}$$

The modified compression index λ^* is expressed in equation (2.5). A compilation of all the parameters used in the creep-SCLAY1S model is found in the appendix A.

5 Results

In this chapter, results are presented from the simulations performed in 2D Plaxis on a number of excavation and embankment problems with set of parameters from the mini block and piston (STII) sampler. By using the User-Defined Soil Model (UDSM), creep-SCLAY1S, the results is simulated and then analysed to check the long-term behaviour of the silty clay/clayey silt underneath the considered geotechnical construction.

5.1 Initial consolidation & OCR dependency

In order to establish the initial consolidation in the soil an analysis is performed with the creep-SCLAY1S model before any geotechnical construction is applied. The soil has deposited due to sedimentation and seasonal variations for thousands of years which implies that some degree of anisotropy has been developing in the soil. This is decisive of how much over-consolidation that has occurred in the soil layers. In the models the coefficient of earth pressure for over-consolidated clay K_0 is set to 0.6. The OCR value measured from the mini block samples has a ratio between 1.45-1.5 and the piston (STII) case a ratio between 1.25-1.3.

However, 100 years is selected in interest of analysing the background creep that has been developing in the soil. This is presented in figure 5.1 for the piston (STII) and mini block case. The magnitude of background creep differs significantly between the samples due to the difference in OCR value. Reason for the difference is that the piston (STII) case is more exposed to disturbance during field sampling. According to Mats Karlsson et al. (2015) draft report the classification of sample disturbance based on equation (2.15) ranges between "excellent to very good" for the majority of the samples.

The magnitude of the OCR has a large influence on the creep rate $\dot{\Lambda}$. It also affects K_0 which controls the degree of elastic and plastic deformations that have taken place in the soil, however as was mentioned above, K_0 is set to 0.6 for all models.
To understand how much both sample parameters influence the background creep, the creep rate $\dot{\Lambda}$ is determined. This is done by using equation (4.1) defined in chapter 4.3 about the creep-SCLAY1S model. The OCR can be incorporated in the equation by setting $p'_{eq}/p'_{mi} = 1/OCR$
The creep ratio β is defined by equation (3.25). Table 5.1 shows that the creep rate differs significantly between the two sample parameters.

Table 5.1: Initial consolidation, Creep rate and Creep ratio determined from the mini block and piston (STII) sampler parameters

Sampler	OCR	Creep ratio β	Creep rate $\dot{\Lambda}$
Mini block	1.45	65.6	$5.11 \cdot 10^{-14}$
Piston (STII)	1.25	61.6	$2.11 \cdot 10^{-8}$

The piston (STII) case in figure 5.1 shows that the background creep decreases slowly exponentially with time and after 100 years the soil has settled about 0.028 meters which corresponds to 0.28 mm/year.

The background creep represented in figure 5.1 for the mini block case is almost non-existent, nearly no creep develops in the soil.
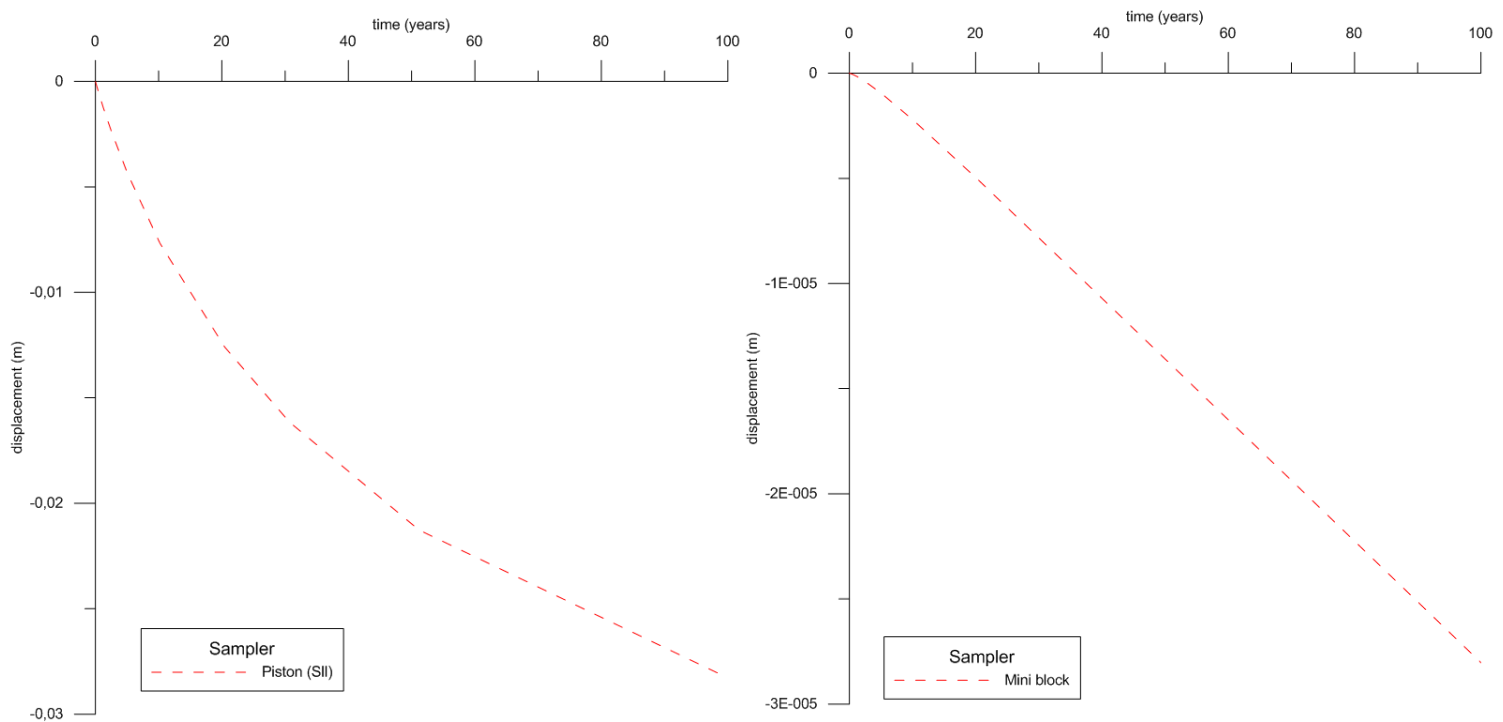

Figure 5.1: Initial consolidation after 100 years of creep before the embankment/excavation have been constructed for the mini block (left) and piston (right) case

5.2 Embankment – Vertical & horizontal displacement for different heights

The vertical and horizontal displacement showed in figure 5.2 and 5.3 is generated by applying an embankment load on top of the soil layers. This is performed for the embankment heights one, two and three meters. All models are assumed to have a fixed slope inclination with the ratio 1:3. An embankment figure is plotted above to illustrate how the displacement relate to the embankment layers. The consolidation goes on for 100 years and is performed for both the mini block and piston (STII) case to observe the effect of using high quality samples in a long-term perspective.

The piston (STII) case results in larger displacement contra the mini block case due to its lower OCR value, see appendix A for a compilation of the parameters. It should also be mentioned that the dry crust layer contributes to a lower displacement in the underlying silty clay/clayey silt layers due to its relatively high stiffness.

Figure 5.2 shows the vertical displacement provided by a horizontal cross section measured two meters beneath the ground surface in the model. Solid lines represent the displacement developed from the mini block parameters and dashed lines from the piston (STII) parameters. Maximum displacement occurs as predicted underneath the centreline of the embankments. For the first meter embankment the divergence is about 53% between the mini block and piston (STII) case, for two meters 38% and three meters 35%.

The horizontal displacement in figure 5.3 is measured from the embankments toe crest to a depth of 20 meters. Maximum horizontal displacement occur in-between the dry crust layer and the first silty clay/clayey silt layer located at two meters depth below ground surface. This is also the location of the groundwater level, see figure 4.2. The difference in horizontal displacement between the mini block and the piston (STII) sampler is 44% for one meter embankment, 37% for two meters embankment and 37% for three meters embankment.
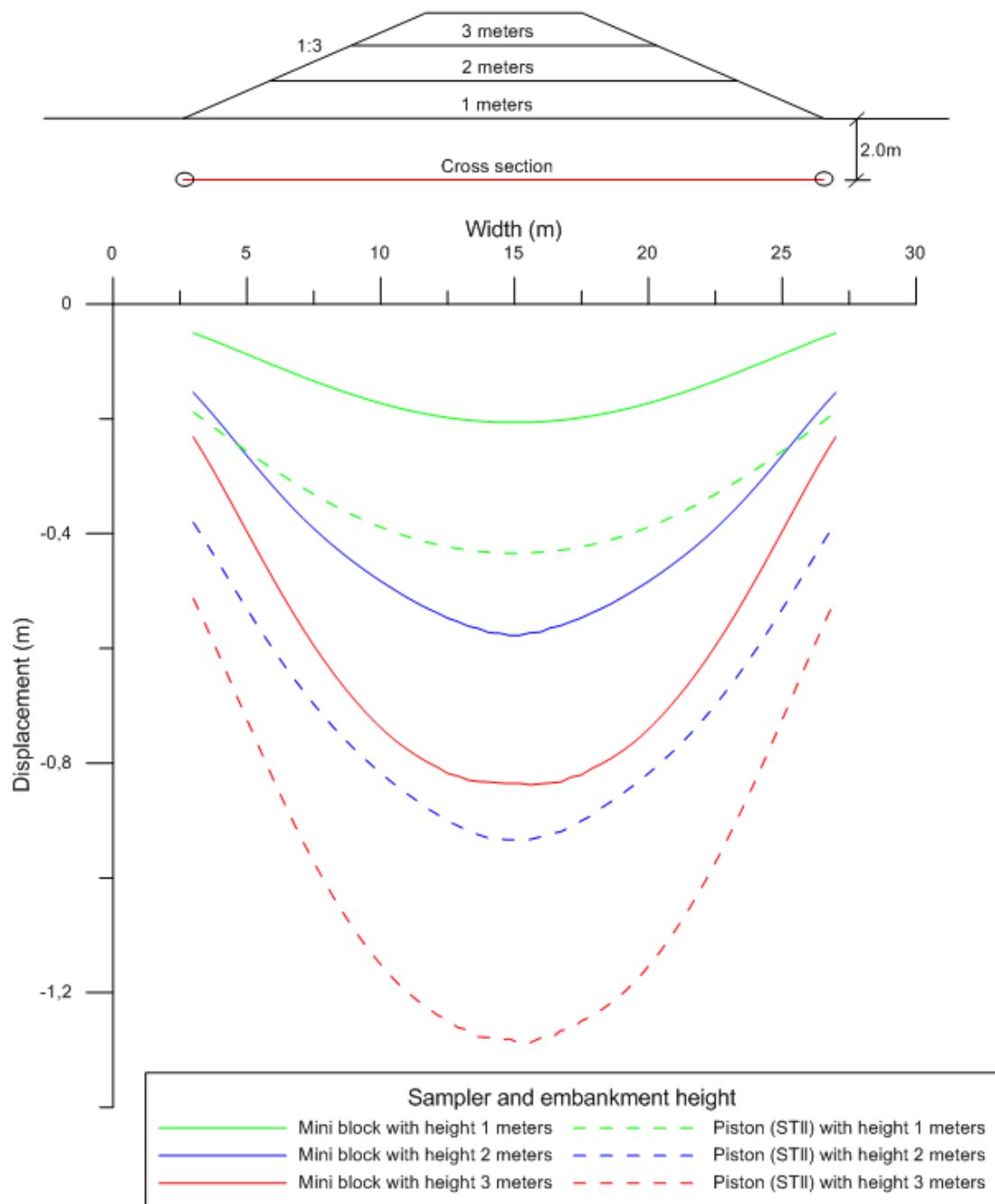
Figure 5.2: Vertical displacement measured two meters beneath the embankment for both the mini block and piston (STII) case for different embankment heights after 100 years
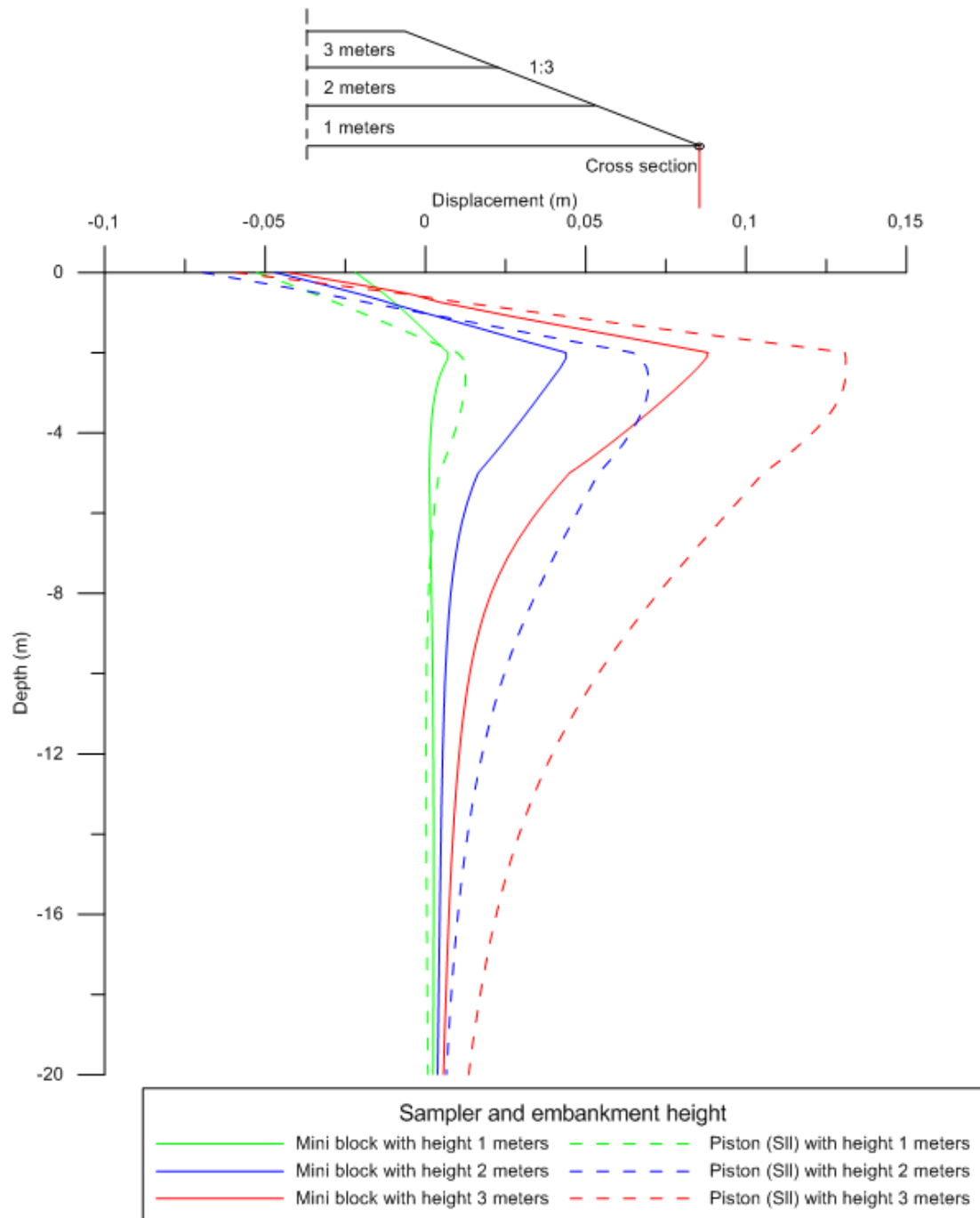
Figure 5.3: Horizontal displacement measured from the embankments toe crest to a depth of 20 meters for both the mini block and piston (STII) case for different embankment heights after 100 years

5.3   Embankment – Vertical deformation & pore pressure against time

Figure 5.4 represent the vertical displacement that occurs after embankment construction at different stages during consolidation. In the models a horizontal cross section is performed two meters beneath ground surface as is illustrated in the figure. For this problem a two meter high embankment is constructed on top of the soil layers. Smaller time step is assumed for the first years of consolidation since the pore pressure is assumed to dissipate at a faster rate. Already after one year of consolidation, significant vertical displacement is observed in the analyzed clay section. Right after, one year after, five years after and ten years after the embankment is constructed the difference in vertical displacement between the mini block and the piston (STII) case is all 28%. Then after 50 and 100 years, it increases to 36% and 38%, respectively.

The change in excess pore pressure over 100 years is shown in figure 5.5 at six meter depth below ground surface under the centreline of the embankment. This is performed for both the mini block and piston (STII) case for different embankment heights.
In the model the hydraulic boundaries is set as open both in the bottom and in the top to allow seepage in both directions. For all embankment cases the majority of the excess pore pressure has dissipated after 20-30 years which indicate that the deformations that develop at this stage are mainly creep deformations.
Figure 5.5 also shows that lower embankment height build up less excess pore pressure which result in a considerable faster primary consolidation phase that transition into secondary consolidation. The mini block parameters as expected contribute to a faster dissipation of the excess pore pressure then the piston (STII) due to higher OCR value.

By looking at figure 5.4 together with the dissipation of excess pore pressure from the two meter embankment case (blue lines) in figure 5.5, it is observed that large creep deformations occur between the years 10-50, where almost no excess pore pressure remains but still contribute to large deformations. However between 50-100 years the creep deformations has decreased significantly, especially for the mini block case. Note that the creep deformations in figure 5.4 are assumed to be developing during the whole consolidation process. In other words the settlement that develops from the primary consolidation is a combination of dissipated excess pore pressure and creep deformations.
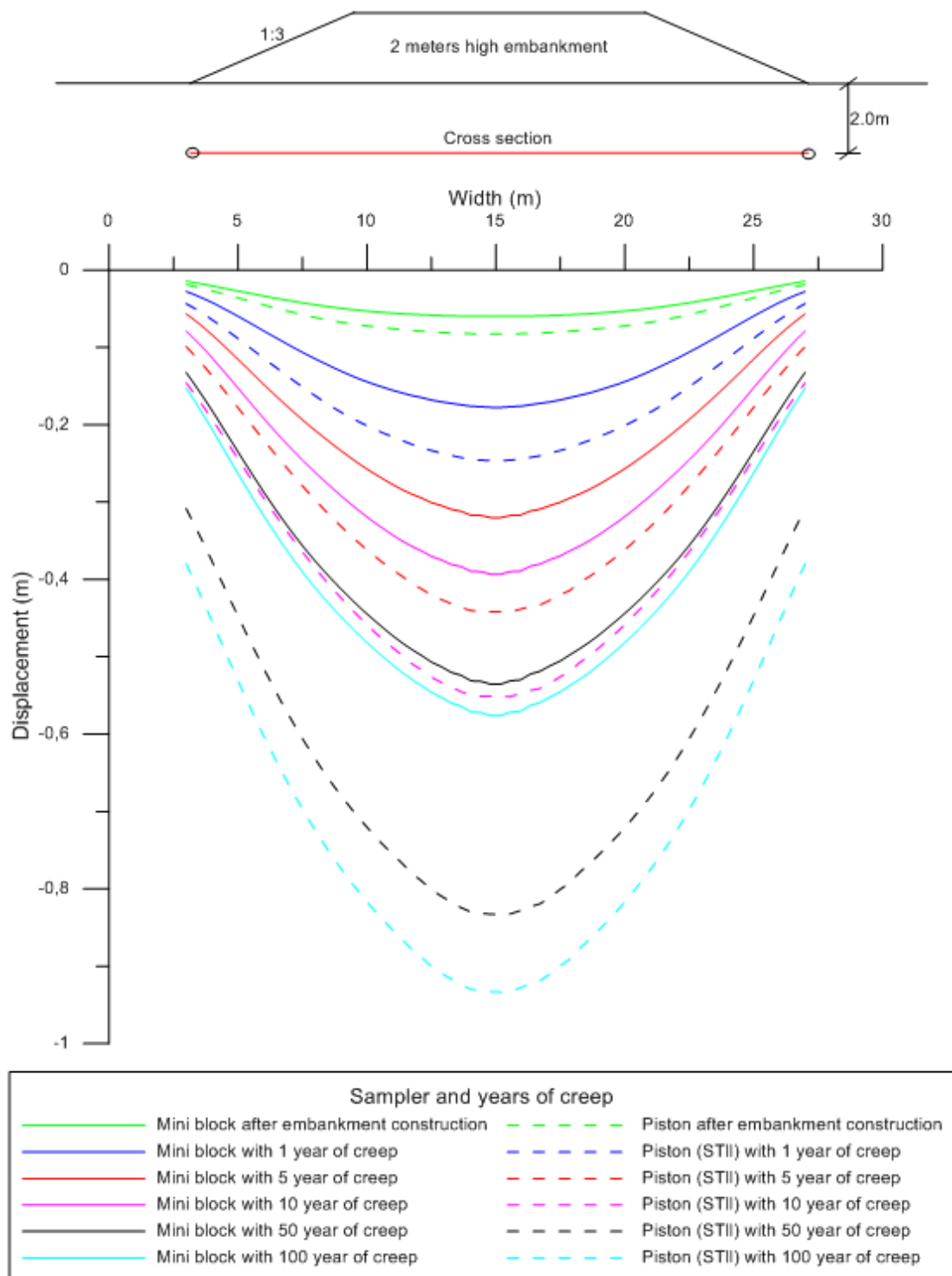
Figure 5.4: Vertical displacement measured after embankment construction two meters beneath ground surface
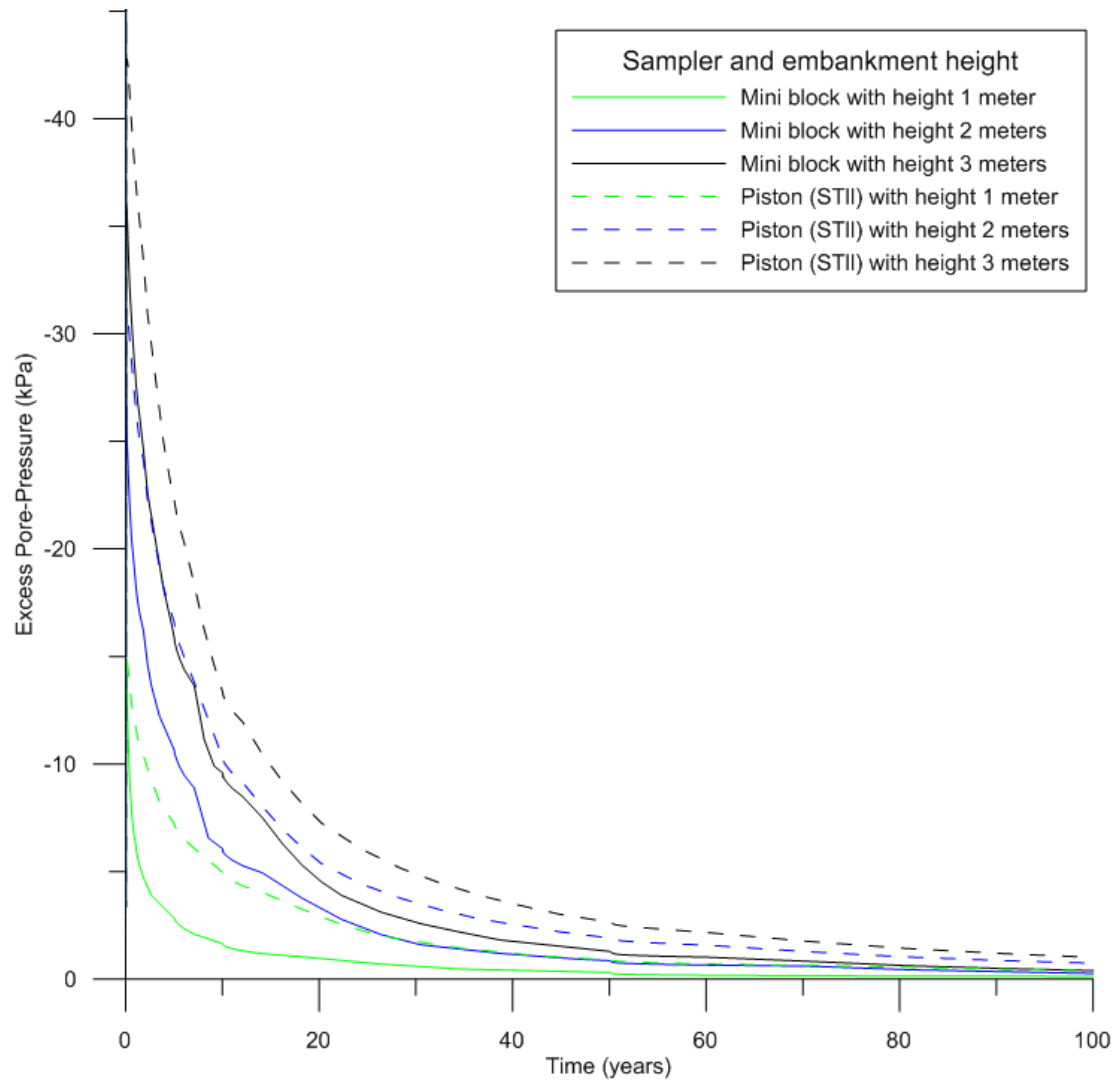
Figure 5.5: Excess pore pressure against time at six meters depth for both mini block and piston (STII) case

5.4 Excavation – Vertical & horizontal displacement for different depths

Excavation problems usually cause the soil to heave where swelling builds up at the bottom of the excavation due to stress relief. Vertical and horizontal displacement is shown in figure 5.7 and 5.8 where different excavation depths is analysed. An excavation figure is plotted above to illustrate how the displacement is in proportion to the excavation layers. All models are assumed to have a fixed excavation slope inclination with the ratio 1:3 and analysed 100 years after construction similar to the embankment problems to analyse high quality samples in long-term perspective.

Figure 5.8 shows a horizontal cross section performed at 3.5 meters depth in the model to determine the vertical displacement underneath the excavation. As predicted a larger un-loading of soil causes larger vertical displacement where maximum displacement occurs at the centreline of the excavation. Regarding the one meter excavation case a rather small difference in displacement is observed. For the other excavation cases at two and three meters depth a considerably higher differentiation between the sampler parameters is observed.

The horizontal displacement is determined in the excavations toe crest on the right hand side to 20 meters depth and is presented in figure 5.9. Relatively small horizontal displacement has developed after 100 years, particularly regarding the mini block parameters. One of the main reasons for this is that the first 2 excavation meters is constructed in the dry crust layer which counteract that large horizontal displacement builds up in the underlying silty clay/clayey layers due to its high stiffness.

Regarding the excavation case at three meters depth in figure 5.8 and 5.9, negative pore pressure builds up underneath the excavation. This causes local spikes to emerge from the soil layers in the models. To prevent this, a small strip is added underneath the last excavation layer beneath the groundwater level that is set as dry in combination with an interpolation of the pore pressure for the first clay layer in order to prevent the local spikes. By doing this the measured displacements should be accurate to what is expected without these local errors.

Similar to the embankment case, vertical displacement against time is analysed for a two meters excavation and is shown in figure 5.11. A large increase in displacement is observed already after one year of consolidation. However, after five years the vertical displacement decreases drastically and between 50 years no creep deformations develops for either sampler case. It is however noticeable that there is a substantial difference between the mini block and piston (STII) parameters.

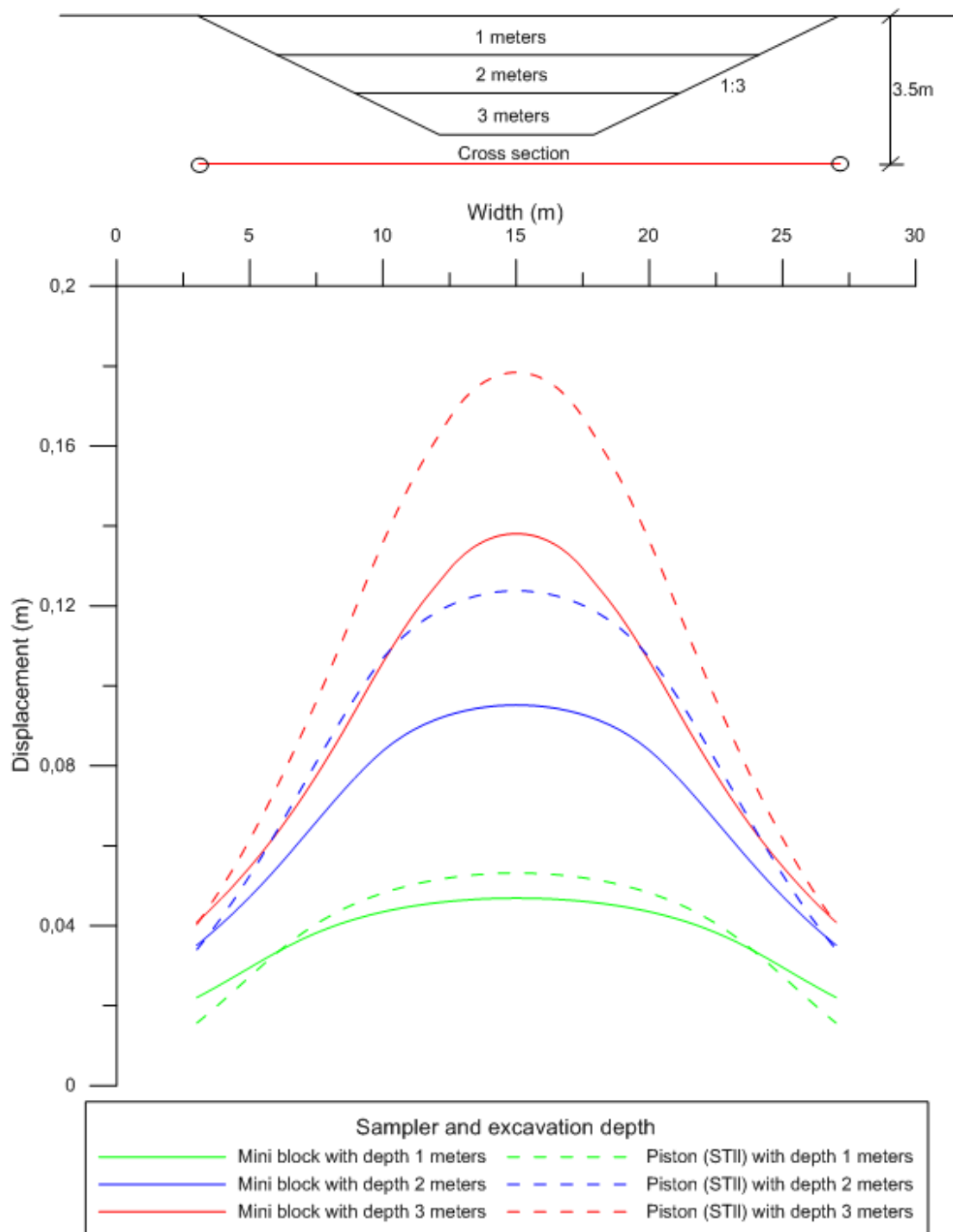*Figure 5.7: Vertical displacement measured 3.5 meters beneath the ground surface where both mini block and piston samples (STII) at different excavation depths after 100 years is analysed*
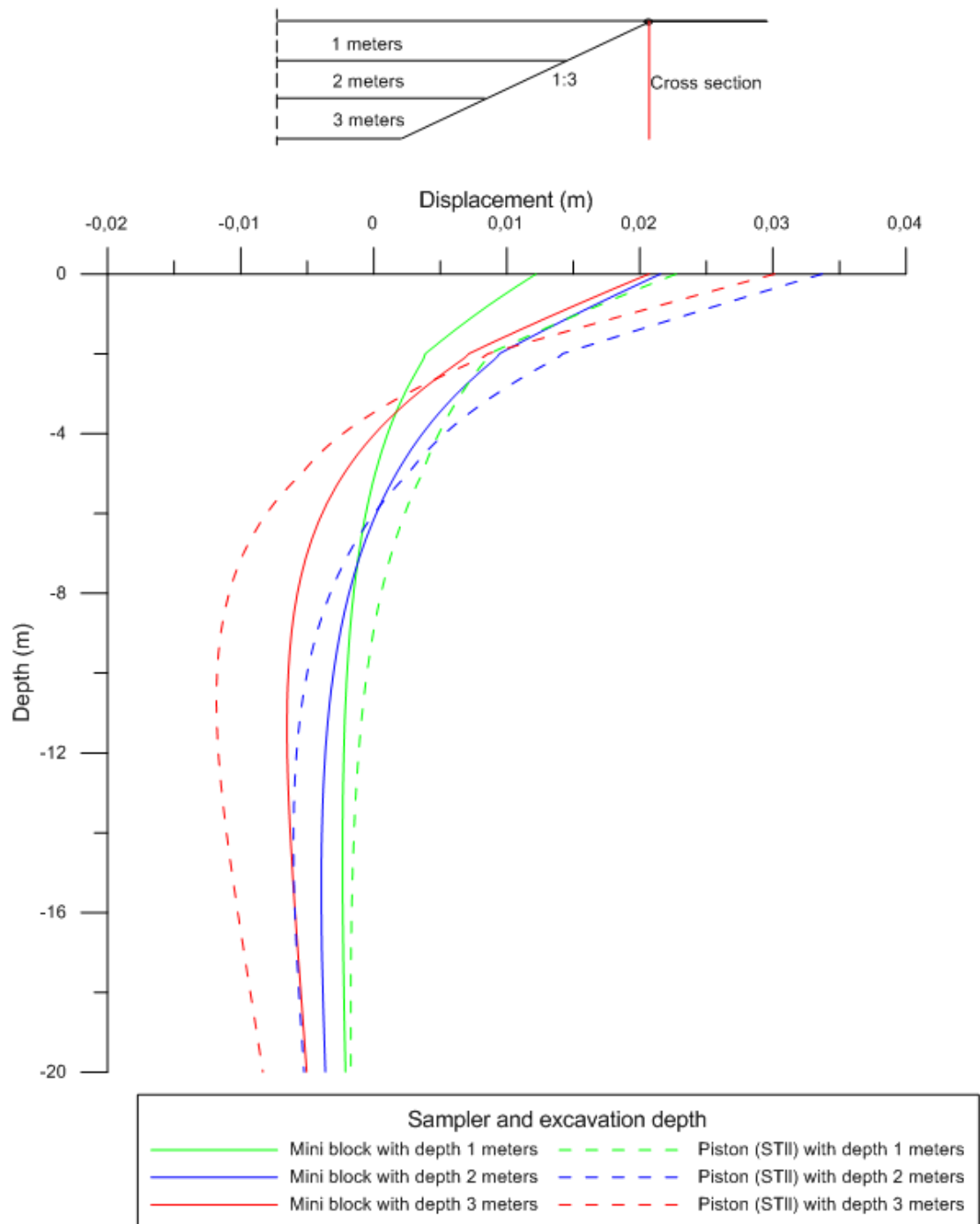
Figure 5.8: Horizontal displacement measured from the toe of the excavations slope to a depth of 20 meters is analysed for both the mini block and piston (STII) case at different excavation depths after 100 years
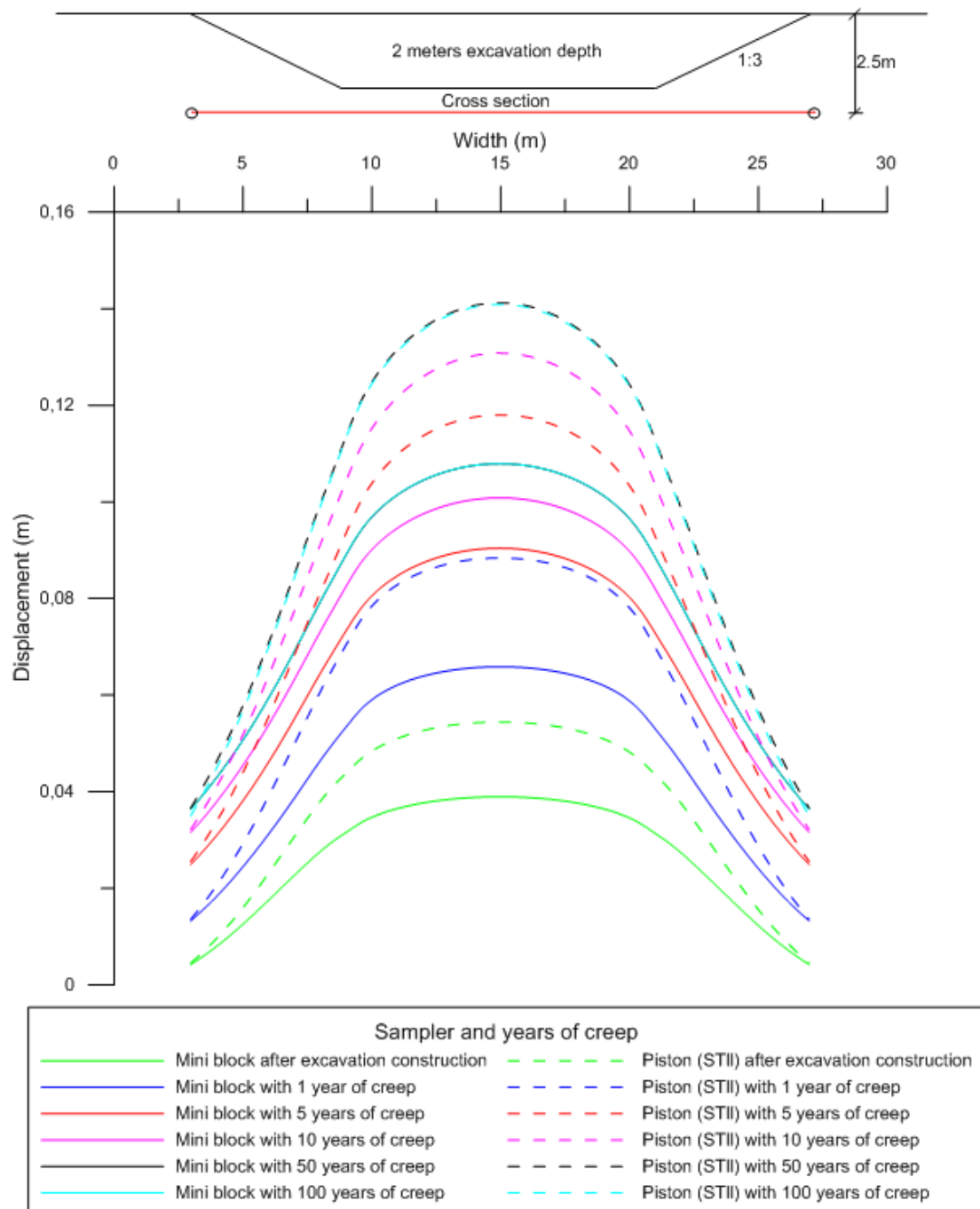
Figure 5.11: Vertical displacement measured after excavation construction 2.5 meters beneath ground surface for different time steps

5.5   Excavation – Vertical & horizontal displacement for different slopes

Steeper slopes in regard to unloading problems generally generate larger vertical and horizontal displacement but do require less excavation procedure. In this case a two meters excavation is constructed as illustrated in figure 5.9 and 5.10 where the slope inclinations 1:2, 1:3 and 1:4 are analysed. As in previous problems consolidation is performed for 100 years after the excavation is constructed for both the mini block and piston (STII) case. For unloading problems the modified swelling index κ^* has a larger influence contra the embankment problems. The mini blocks modified swelling index is set to 0.15 and the piston (STII) is set to 0.2 where a lower value contributes to higher stiffness in the clay layers and vice versa.

In figure 5.9 the vertical displacement is measured 2.5 meters beneath ground surface. A steeper slope generates larger vertical displacements both in the middle and on the sides of the analysed excavation, especially for the piston (STII) case. The increase in displacement also appears to be close to constant between the analysed slope variations. Hence, the difference in vertical displacement between all the mini block and piston (STII) cases is 24%. Once again it is established that the OCR has a remarkable influence on the simulations.

The horizontal displacement in regard to different slope inclinations is investigated at the toe crest of the excavation and is analysed to a 20 meters depth which is illustrated in figure 5.10. Observations make it clear by comparing the horizontal displacement between the slope inclinations that no significant increase occurs between the mini block and piston (STII) parameters. Around five meters depth the horizontal displacement is equivalent for both cases. The maximum horizontal displacement in the silty clay/clayey silt is located at approximately 13 meters depth.

By this information, it is confirmed that excavation depth and slope inclination plays an important role when it comes to the magnitude of heave in slightly over-consolidated clay.
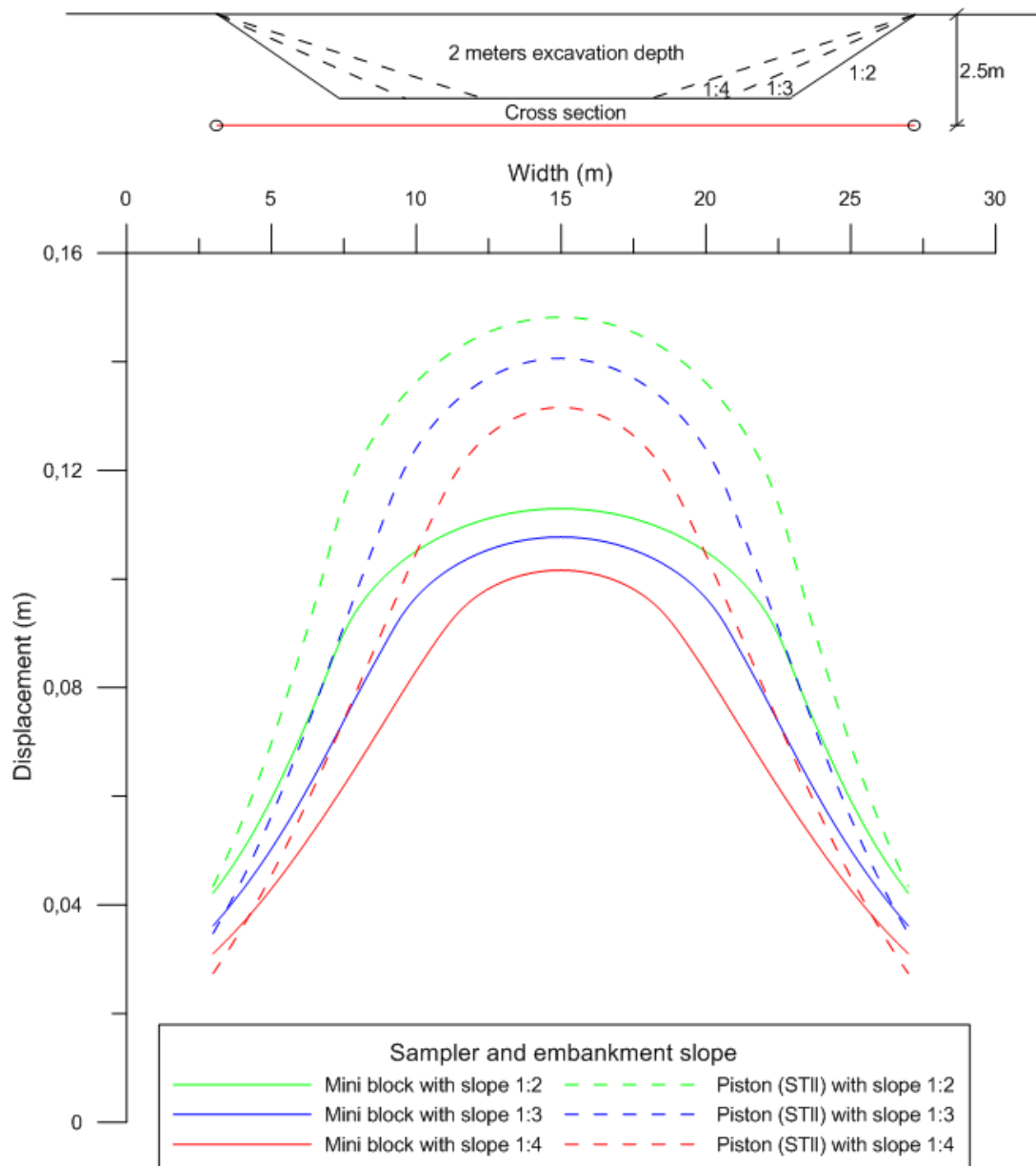
Figure 5.9: Vertical displacement measured 2.5 meters beneath ground surface for a fixed embankment height at two meters with different slopes after 100 years
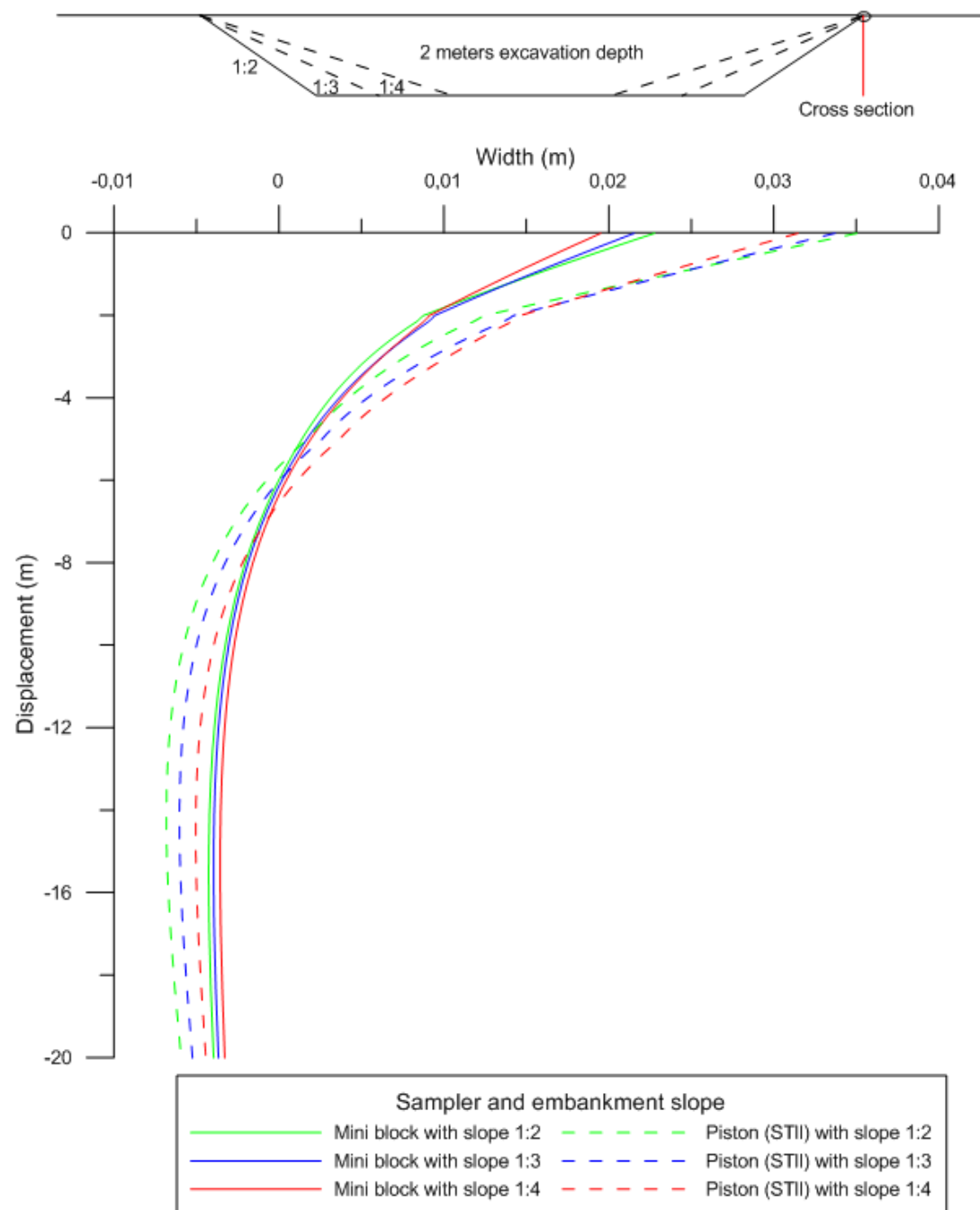
Figure 5.10: Horizontal displacement measured 2.5 meters beneath ground surface for a fixed embankment height at two meters with different slopes after 100 years

6 Credibility assessment

To analyse the credibility of the results in chapter 5 a sensitivity analyse is performed. Furthermore the impact of anisotropy and destructuration is evaluated by setting the parameters that are associated to zero. A stress analysis is also performed for the embankment case. At last shear strength at different soil depths is established.

6.1 Sensitivity analysis

Since the OCR value is highly influenced by disturbance during field sampling, a sensitivity analysis is carried out to check the OCR dependency for the silty clay/clayey silt when a two meters high embankment is constructed above the soil layers. Only the piston (STII) parameters are used to perform the sensitivity analysis by incorporating different OCR values. Figure 5.14 illustrate how the vertical displacement is dependent of the analysed OCR values. A lower OCR will obviously generate in larger vertical displacement underneath the embankment. The displacement is measured with a horizontal cross section two meters beneath the ground surface as is illustrated in the figure.

Table 3: Sensitivity analysis, Creep rate and creep ratio determined from the piston (STII) sampler parameters

OCR	β	Creep rate
1.45	61.6	$2.26 \cdot 10^{-13}$
1.35	61.6	$1.85 \cdot 10^{-11}$
1.25	61.6	$2.11 \cdot 10^{-8}$
1.15	61.6	$3.59 \cdot 10^{-7}$
1.05	61.6	$9.76 \cdot 10^{-5}$

The OCR value, as has been established earlier in this MSc thesis, has a large influence on the creep rate $\dot{\Lambda}$. Table 3 shows the calculated creep rate for the OCR values plotted in figure 5.14. Equations (4.1) and (3.25) are used to calculate the expected creep rate $\dot{\Lambda}$ and creep ratio β. As the creep rate indicates, the total deformations show a larger rate of increase for lower OCR values. The vertical displacement shown in figure 5.14 increases by 22% between the OCR values 1.35-1.45, 25% between 1.25-1.35, 27% between 1.15-1.25 and 28% between 1.05- 1.15.
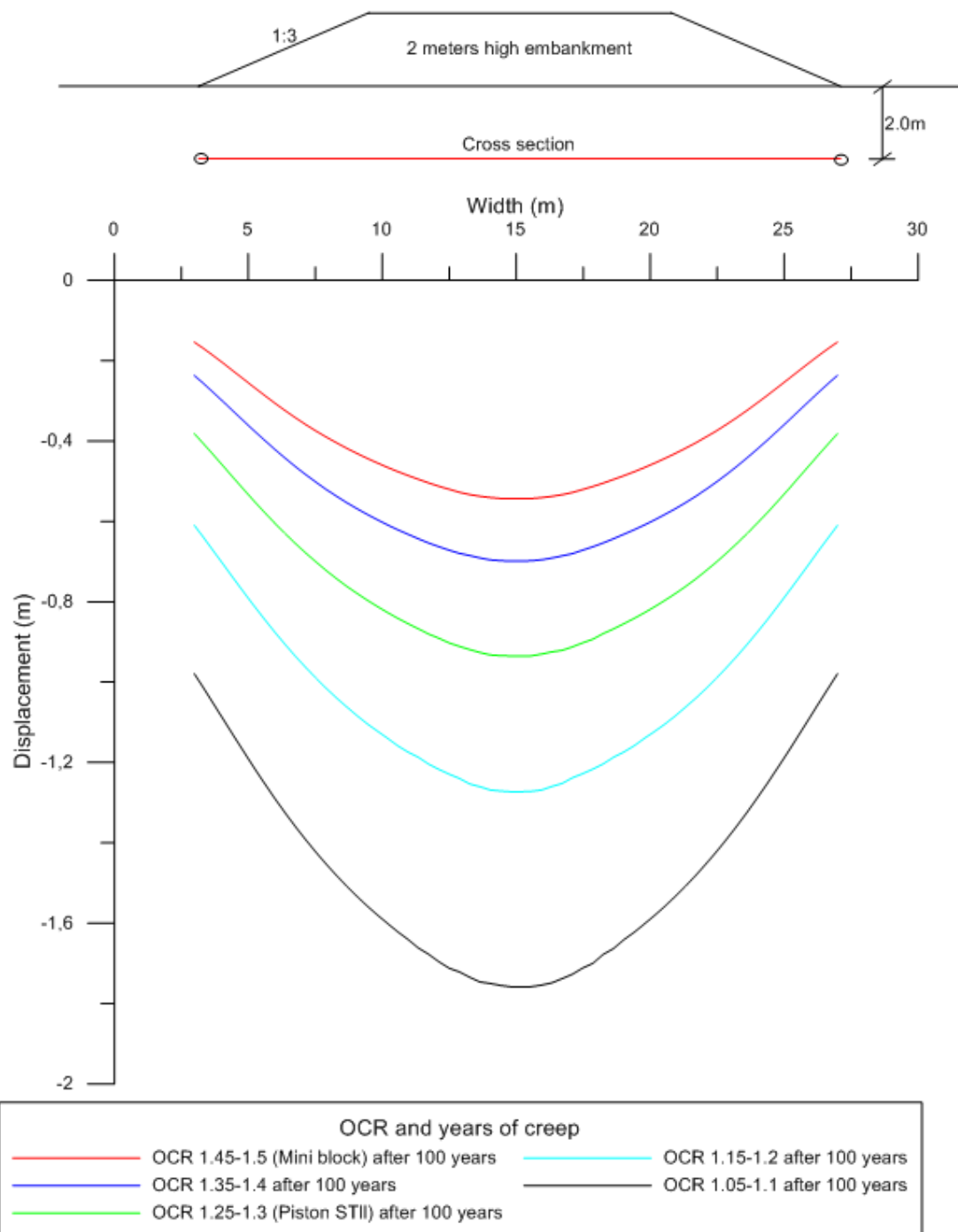
Figure 5.14: Sensitivity analysis performed for a variation of OCR values regarding the piston (STII) parameters where vertical displacement is measured two meters beneath the ground surface after 100 years of creep

6.2   Anisotropy & destructuration

In interest of analysing the effect of anisotropy in the creep-SCLAY1S model, test simulations in which the rotational hardening laws ω and α is set to zero. By ignoring the evolution of anisotropy the settlements in both vertical and horizontal direction is underestimated and it's thereby essential to involve the anisotropy in order to provide a realistic outcome. The reason is that the model for this particular case predicts higher soil stiffness when the evolution of anisotropy and destructuration is set to zero. In order to study the effect of including destructuration, the bonding parameter χ is set to zero.

In figure 5.12 the dependency of anisotropy and destructuration shown after embankment construction is completed (left) and after 100 years (right). This is done for a two meters high embankment with a fixed slope inclination at 1:3. The effect of anisotropy and destructuration has a large influence the first year, see appendix B1. After that it only has a marginal effect. Without anisotropy a slight decrease in displacement is observed. Largest influence has the destructuration, when χ is set to zero where a significant decrease in displacement after 100 years is observed. By ignoring both the anisotropy and destructuration, the vertical displacement after 100 years is 63% in relation to when the parameters are activated.

The anisotropy and destructuration dependency is also analysed for the excavation problem. In figure 5.13 the vertical displacement is presented for a two meters deep excavation. Same conditions are used for the excavation as where done for the embankment problem. For the excavation case the influence of destructuration is non-existent and the anisotropy only provide a small effect on the overall displacement. A compilation of the anisotropy and destructuration dependency of the excavation is seen in appendix B2.
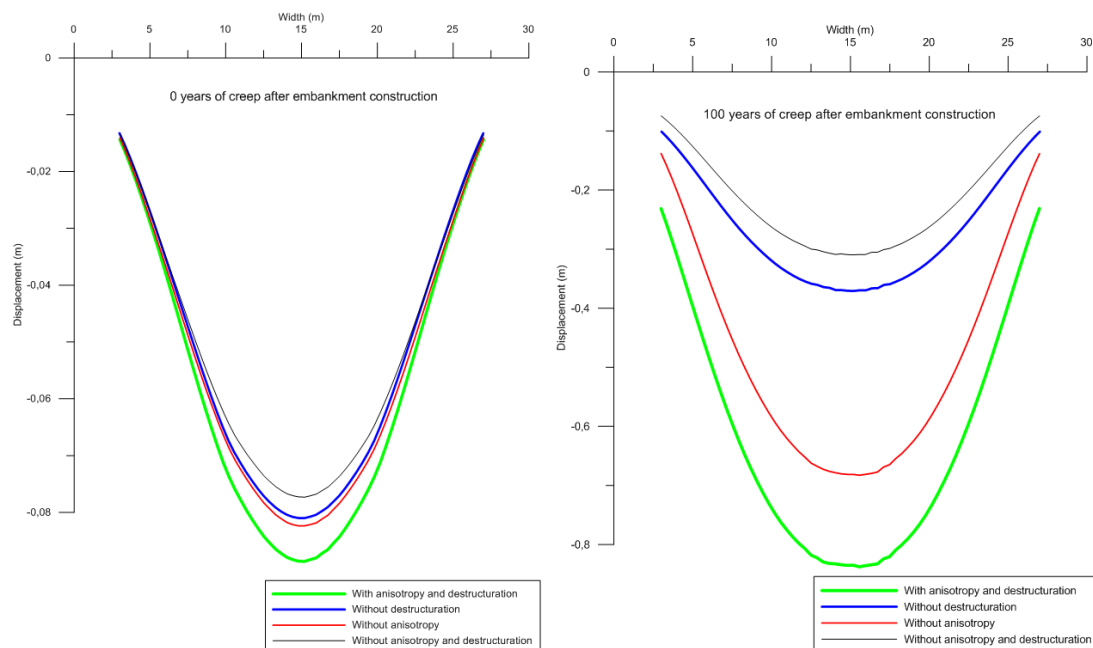

Figure 5.12: Vertical deformation after embankment construction and after 100 years with and without anisotropy and destructuration
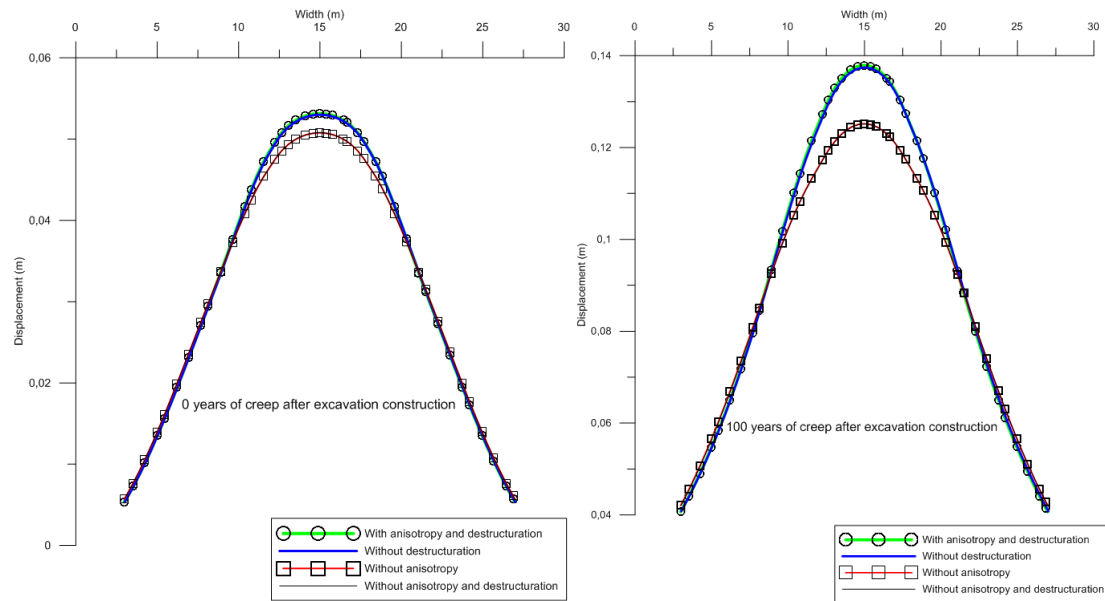
Figure 5.13: Vertical displacement after excavation construction and 100 years with and without anisotropy and destructuration

6.3   Stress analysis

Another way to describe the behaviour in the soil layers is to represent stresses against depth. This is done by using two well-proven methods to get an insight how the pre-consolidation pressure relate to the in-situ stresses and stresses developed from the embankment. Figure 5.6 and 5.7 represent the in-situ vertical effective stress σ_v', pre-consolidation pressure p_c' for both sampler cases and the stresses after embankment construction $\sigma_v' + \Delta\sigma_v$ against 20 meters depth.
The chosen embankment height for this analysis is two meters that weight 20kN/m^3 which corresponds to about 40kPa.

In figure 5.6 the first acclaimed method is used. If the stresses from the embankment (red line) exceed the pre-consolidation pressure (blue and green line) from either sampler case, plastic deformation is bound to transpire. For the mini block case this is assumed to occur till a depth of 8.5 meters and the piston (STII) case 16 meters before the pre-consolidation pressure becomes greater than the stresses from the embankment. The stress difference at two meters depth between the embankment and the pre-consolidation pressure for the piston (STII) case is 45% and 36% for the mini block case. Notice that the embankment stresses at this depth is uncertain and an average value is considered.

The second method is to look at 0.8 times the pre-consolidation pressure to verify if creep needs to be further evaluated. Studies have showed that $p_c' \cdot 0.8$ is an indicator whether the influence of creep should be considered or not. If $\sigma_v' > p_c' \cdot 0.8$ it is acceptable to ignore the predicted creep, but if $\sigma_v' < p_c' \cdot 0.8$ considerable creep is predicted to develop and needs to be investigated for the problem at hand. This method is represented in figure 5.7 to establish whether the mini block or piston (STII) parameters fulfils this criterion or not. It is observed that the $p_c' \cdot 0.8$ for the

piston (STII) case is on the verge to exceed the in-situ vertical stress σ_v'. Nevertheless, neither of the samplers needs to consider the influence of creep deformation based on this method.

These methods is however simplified and only take into account vertical stresses which do not give a justified outcome since there are generally a lot of factors that need to take into consideration to determine a soils behaviour. They give however some proportion at what stress levels the deformations is expected to develop.
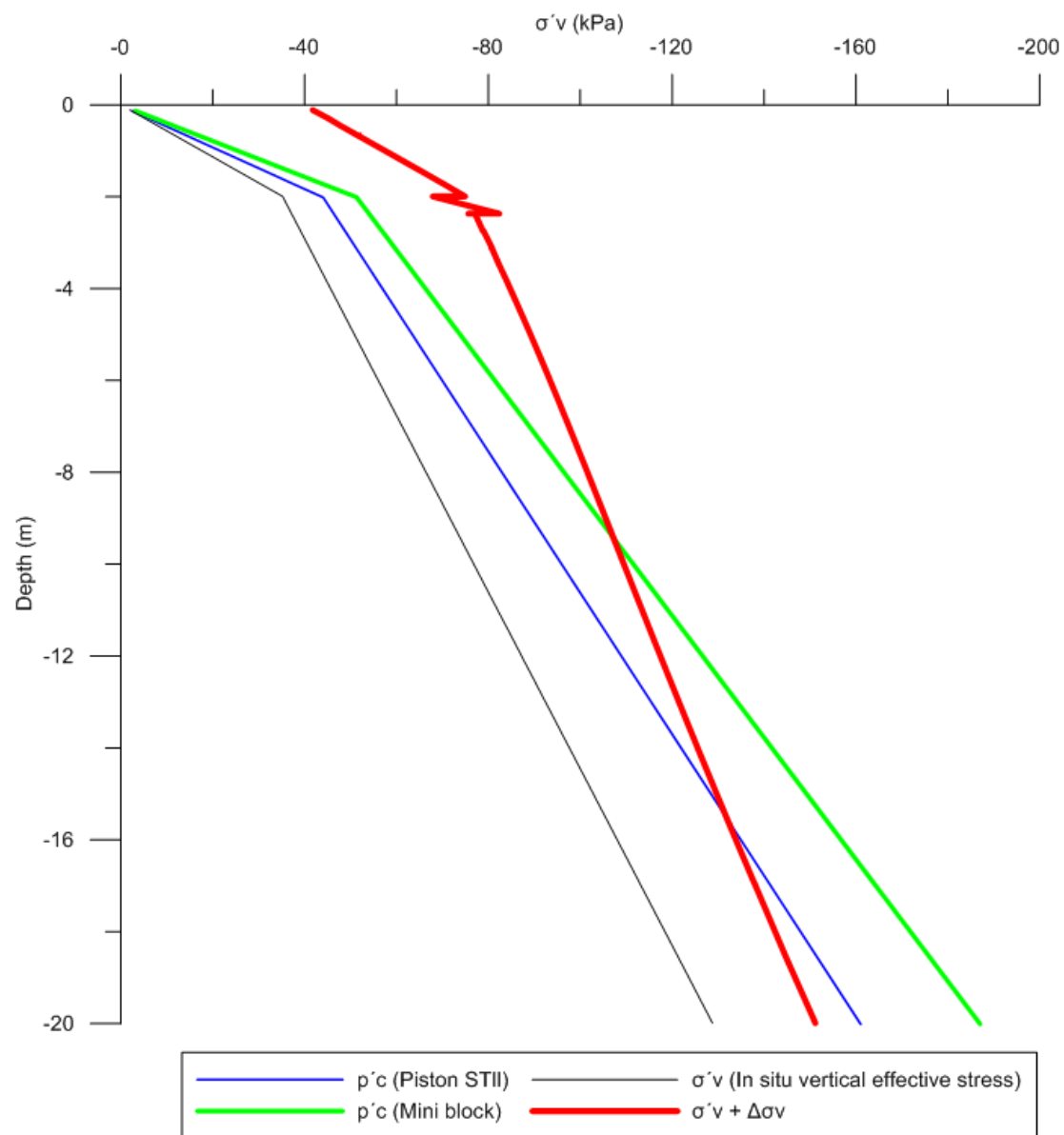
Figure 5.6: In-situ vertical effective stress, pre-consolidation pressure and stresses from the embankment plotted against depth
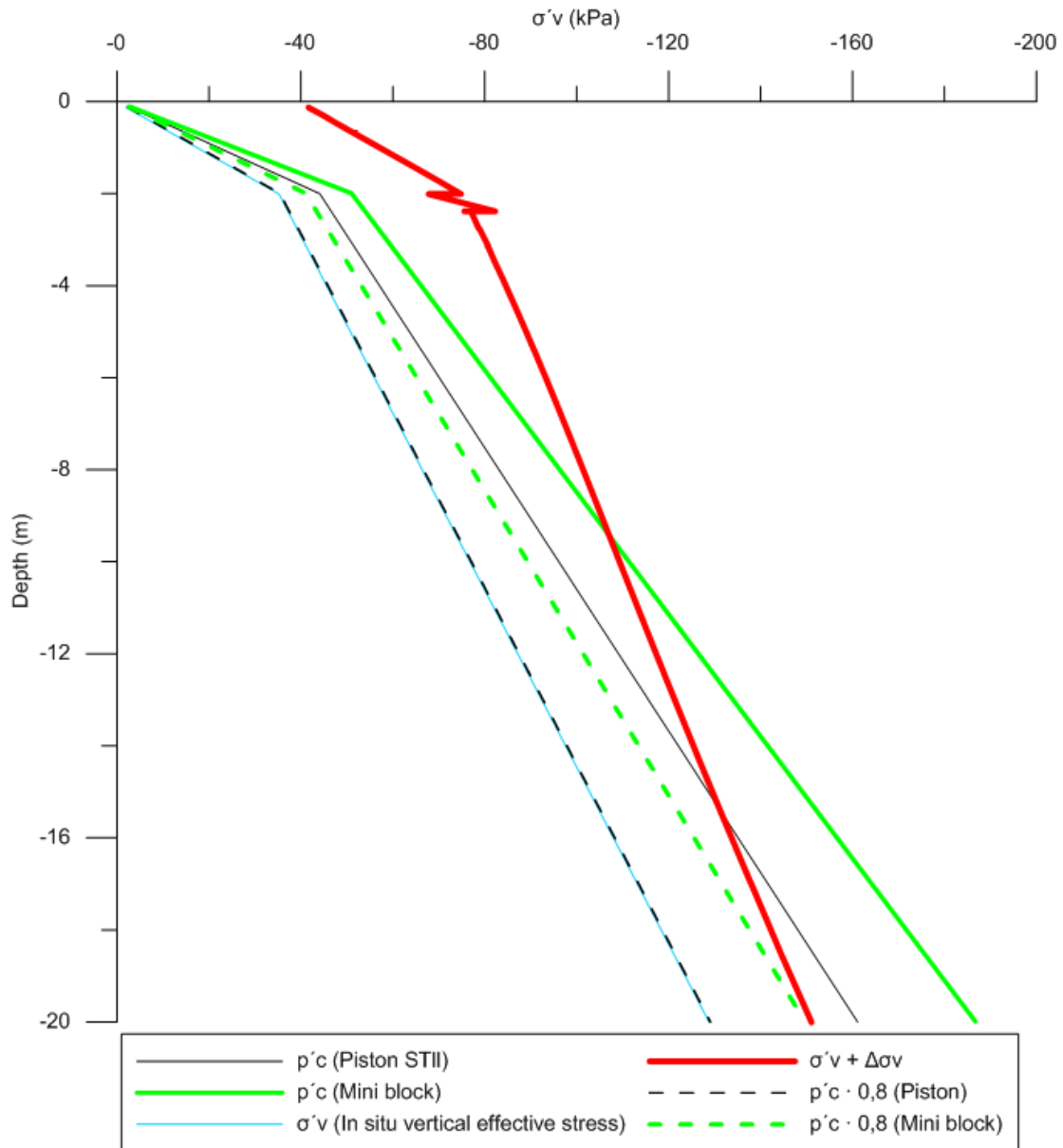
Figure 5.7: In-situ vertical effective stress, pre-consolidation pressure times 0.8 and stresses from the embankment plotted against depth

6.4 Initial active & passive shear strength

To establish the initial active and passive shear strength the SoilTest tool where used in 2D Plaxis. This is done in order to validate whether the initial active and passive shear strength in the creep-SCLAY1S model is reasonable and to compare it to the lab measurements presented in *Mats Karlsson, Anders Bergström* and *Jelke Dijkstra* technical draft report. Triaxial compression and extension tests are simulated to analyse the shear strength at different depths. In order to do so the horizontal effective stress $\sigma_3^{'}$ is established between the soil layers. When the radial effective stress is larger than vertical effective stress in the triaxial test a negative outcome on the y-axis is assumed, this is the condition indicative of extension and passive shear strength.

In table 4 a compilation of active and passive shear strength for the clay layers is established. To get a perception of the chosen locations, check figure 4.2 in previous chapter. The Coefficient of earth pressure in-situ K_0 is set to 0.6 for all the clay layers and uses undrained conditions. These predictions of the undrained active and passive shear strength based on the creep-SCLAY1S model correspond well to the triaxal tests presented in Mats Karlsson et al. 2015 technical draft report.

Table 4: Active and passive shear strength at different depths

Soil layer	Depth [m]	σ_3' [kPa]	K_0 [-]	C_u(active) [kPa]	C_u(passive) [kPa]
Clay layer 1	2.0	21.8	0.6	16.0	10.2
Clay layer 1-2	5.0	30.5	0.6	22.3	14.3
Clay layer 2-3	12.0	52.4	0.6	38.4	24.5
Clay layer 3	40.0	139.7	0.6	102.0	65.3

Figure 5.16 represent the active and passive undrained shear strength at 5 meters depth. A larger horizontal effective stress σ_3' generates in an increased Mohr surface as is showed in the figures. The Mohr surface defines the magnitude of the active and passive undrained shear strength. A failure envelope is plotted as a straight line since undrained conditions is assumed. The remaining results are compiled in the appendices C1 and C2.
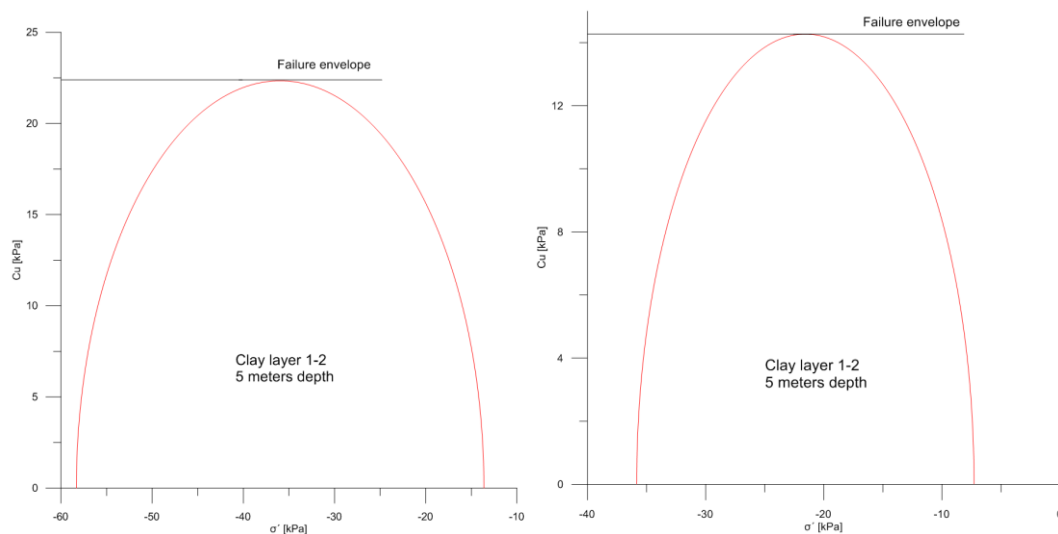

Figure 5.16: Active undrained shear strength (left) and passive undrained shear strength (right) at five meters depth

7   Discussion

In the case of geotechnical numerical modelling there is always some assumptions and simplification in the estimation of input values. Thereby it´s difficult to evaluate the accuracy of the calculated simulations in the models. Still, this is something that needs to be done.

It could be argued why the measured coefficient of earth pressure for over-consolidated clay K_0 (see appendix A) assumed from *Mats Karlsson, Anders Bergström and Jelke Dijkstra* (2015) technical draft report, differs with simple calculations based on Schmidt´s equation (2.4). A much higher OCR value would be needed in order to acquire same K_0 value from their measurement. However, this doesn't exclude that the measurements is accurate, only that it's high in relation to the calculated value.
The friction angle for the silty clay/clayey silt is estimated to 39.2°. This is not a standard value in these kinds of soils in regard to less sophisticated methods in the industry and is generally set as a lower value around 30°. Such high friction angle as 39.2° results in lower K_0 value and higher undrained shear strength that normally would be the case for lower friction soils.

Another uncertainty in this MSc thesis is the mesh dependency in the models. A convergence check could be performed in order to validate that the right number of elements was used for the models. The decision behind using 6-noded elements in prior to 15-noded elements is due to issues regarding the pore pressure. The addition of creep in the creep-SCLAY1S model causes numerical fluctuation, which triggers additional excess pore pressure. 15-nodel elements is more accurate when only consolidation is involved, however when also creep is incorporated 6-noded elements is to be preferred.

The majority of the results are heavily influenced by the effect of the OCR between the mini block and piston (STII) case which is inarguably the most important parameter. This is nevertheless not the only parameter that affects the results. The magnitude of the modified index parameters λ^* ,κ^* and μ^* for example could have been studied more in detail by performing sensitivity analyses.

It could also be argued to what degree the dry crust layer contributes to the total displacement in the underlying silty clay/clayey silt layers. An interesting aspect would be to remove the dry crust and replace it with silty clay/clayey silt to analyse the increased displacement.

In some of the results only one embankment/excavation problem is chosen to be analysed, for example the sensitivity analyze in chapter 6.1. The one meter case is considered to be least favorable to be analyzed. For the two and three meter embankment/excavation cases however, both could be considered equally important.

8 Conclusions & Recommendations

8.1 Conclusions

As is seen in the sensitivity analysis the OCR value has a substantial influence on the overall displacement, where a lower OCR results in an increased creep rate. It can be concluded that using parameters based on high quality samples is essential in determining the vertical and horizontal displacement for this type of soil conditions in regard to embankment/excavation problems. The majority of the piston (STII) cases significantly overestimates the actual deformations compared to the displacement observed from the mini block case.

By looking at vertical long-term displacement against time for 100 years the consolidation process is studied. This made it possible to confirm whether long-term creep is of essence or not by studying the vertical displacement together with the dissipation of excess pore pressure. For the embankment case the displacement continues to develop even after almost all excess pore pressure has dissipated. This entail that at this stage, the soil undergoes pure creep deformations. For the unloading case on the other hand, the displacement stops to develop after 50 years for both the mini block and piston (STII) case. Additionally, in regard to the embankment problems, less excess pore pressure builds up for the mini block parameters which contribute to shorter consolidation.

To verify the effect of anisotropy and destructuration the parameters associated were set to zero in the creep-SCLAY1S model. By doing so, it could be established that a decrease in vertical displacement occurs as the stiffness in the soil increases. The influence of destructuration is especially important for embankment problems when the amount of bonding χ parameter is set to zero. This may have led to a decrease in undrained shear strength, in this MSc thesis however only the initial undrained shear strength is considered and can therefore not be confirmed. For the excavation case, only the anisotropy parameters influenced the the vertical long-term displacement while the destructuration had no contribution and could be neglected.

The undrained active and passive shear strength predictions from the creep-SCLAY1S model corresponds well to the triaxial tests that were presented in the technical draft report by *Mats Karlsson, Anders Bergström* and *Jelke Dijkstra* (2015).

The analysed 1D vertical stress against depth for the embankment case is unrealistic when compared to the results from the simulations. Hence, it should only provide a general understanding of the stress levels in the soil and not be compared in any lager extent to the simulated result.

Overall, it can be concluded that it´s of essence to include long-term creep in order to predict the long-term soil behaviour accurately for geotechnical problems such as embankment and excavation problems in similar conditions for clays that are slightly over-consolidated.

8.2   Further research/recommendations

Proposed recommendations for further research and recommendations in the area:

- Make studies of similar problems with a more common soil, as the clay in this MSc thesis is regarded as high plasticity soft clay which is representative as "difficult" from the Gothenburg region.

- Although the rate dependent model used in this MSc thesis is significantly improved compared to previous models, additional data is still needed to determine the validation of these results.

- Study the active and passive undrained shear strength at different stages of consolidation in regard of long-term creep for similar loading problems studied in this MSc thesis to compare it with the initial undrained shear strength in the clay.

9   References

Ashrafi, M.A.H. (2014). *Implementation of a Critical State Soft Soil Creep Model with Shear Stiffness*. Norwegian University of Science and Technology. Trondheim.

Claesson, P. (2003). *Long term settlements in soft clays*. Chalmers University of Technology. Department of Geotechnical Engineering. Gothenburg, Sweden 2003

Dawd, S., Trygg, R. (2013) *FE analyses of horizontal deformation due to excavation processes in deep layers of soft Gothenburg clay*. Chalmers University of Technology. Department of Civil and Environmental Engineering. Gothenburg, Sweden 2013

Grimstad, G., Degago S.A., Nordal, S., Karstunen, M. (2010). *Modeling creep and rate effects in structured anisotropic soft clays*. Springer-Verlag 2010

Karlsson, M., Bergström, A., Dijkstra, J. (2015). *Comparison of the performance of mini-block and piston sampling in high plasticity clay*. Chalmers University of Technology. Department of Geotechnical Engineering. Gothenburg, Sweden 2015.

Karstunen, M., Krenn, H., Wheeler, S.J., Koskinen, M. and Zentar, R. (2005). *Effect of Anisotropy and Destructuration on the behaviour of Murro Test Embankment*. International Journal of Geomechanics. June 2005, 87-96

Karstunen, M., Koskinen, M. (2008). *Plastic anisotropy of soft reconstituted clays*. NRC Research Press Web

Karstunen, M., Yin, Z.Y. (2011). *Modelling strain-rate-dependecy of natural soft clays combined with anisotropy and destructuration*. AMSS press, Wuhan, China

Koskinen, M., Karstunen M. and Wheeler, S.J. (2002). *Modelling destructuration and anisotropy of a natural soft clay*. Proc 5th European Conference of Numerical Methods in Geotechnical Engineering. P. Mestat, ed., Presses de 1'ENPC/LCPC, Paris, 11-20.

Muir Wood, D. (1990). *Soil Behaviour and Critical State Soil Mechanics*. Cambridge, Cambridge University press

Muir Wood, D. (2004). *Geotechnical modelling*. Spon Press, Taylor and Francis Group. London and New York

Olsson, M. (2013). *On Rate-Dependency of Gothenburg Clay*. Chalmers University of Technology. Department of Civil and Environmental Engineering. Gothenburg, Sweden 2013

Parry, R.H.G. (2004). *Mohr Circles, Stress paths and Geotechnics*. Spon Press, Taylor and Francis Group. London and New York.

Ronald, B.J. Brinkgreve. (1999). *Beyond 2000 in Computational Geotechnics.* PLAXIS B.V, Delft University of Technology, Netherlands

Sivasithamparam, N., Karstunen, M., Bonnier, P. (2015). *Modelling creep behaviour of anisotropic soft soils*. Computers and Geotechnics 69 (2015) 46-57

Wheeler, S.J., Näätänen, A., Karstunen, M. and Lojander, M. (2003). *An anisotropic elasto-plastic model for soft clays*. Can. Geotech. J., 40(2), 403-418.

Appendices
A – Model parameters

Identification	Units	Embankment	Dry crust
Material model	-	Mohr-Coulomb	Mohr-Coulomb
Drainage type	-	Drained	Drained
γ_{unsat}	kN/m^3	19,61	17,65
γ_{sat}	kN/m^3	19,61	17,65
$E^{'}$	kN/m^2	25000,0	7000
$v^{'}$ (nu)	-	0,3	0,3
G	kN/m^2	9615,0	2692
E_{oed}	kN/m^2	33650,0	9423
$c^{'}_{ref}$	kN/m^2	1,0	3,0
$\varphi^{'}(phi)$	°	30,0	30,0
$\Psi \ (psi)$	°	0,0	0,0
k_x	m/day	1,0	1,0
k_y	m/day	1,0	1,0
$K_{0,x}$	-	1,0	0,7

Identification	Units	Clay layer 1	Clay layer 2	Clay layer 3
Sampler case	-	Mini block	Mini block	Mini block
Material model	-	User-defined	User-defined	User-defined
Drainage type	-	Undrained (A)	Undrained (A)	Undrained (A)
γ_{unsat}	kN/m^3	15,2	15,2	15,2
γ_{sat}	kN/m^3	15,2	15,2	15,2
κ^*	-	0,015	0,015	0,015
v (nu)	-	0,2	0,2	0,2
λ^*	-	0,097	0,097	0,097
M_c	-	1,6	1,6	1,6
M_e	-	1,1	1,1	1,1
ω	-	30.3	30.3	30.3
ω_d	-	1	1	1
ξ	-	8,5	8,5	8,5
ξ_d	-	0.3	0.3	0.3
OCR	-	1,45	1,5	1,5
e_0	-	2,0	2,0	2,0
α_0	-	0,636	0,636	0,636
χ_0	-	8,0	8,0	8,0
τ	-	1,0	1,0	1,0
μ^*	-	0,00125	0,00125	0,00125
K_0^{NC}	-	0,368	0,368	0,368
k_x	m/day	0,0000864	0,0000864	0,00006912
k_y	m/day	0,0000864	0,0000864	0,00006912
E_{oed}^{ref}	kN/m^2	30000	30000	30000

c_{ref}	kN/m^2	3,0	3,0	3,0
$\varphi^{'}(phi)$	°	39,2	39,2	39,2
$\Psi\ (psi)$	°	0,0	0,0	0,0
$K_{0,x}$	-	0,6	0,6	0,6

Identification	Units	Clay layer 1	Clay layer 2	Clay layer 3
Sampler case	-	Piston (STII)	Piston (STII)	Piston (STII)
Material model	-	User-defined	User-defined	User-defined
Drainage type	-	Undrained (A)	Undrained (A)	Undrained (A)
γ_{unsat}	kN/m^3	15,2	15,2	15,2
γ_{sat}	kN/m^3	15,2	15,2	15,2
κ^*	-	0,02	0,02	0,02
v (nu)	-	0,2	0,2	0,2
λ^*	-	0,097	0,097	0,097
M_c	-	1,6	1,6	1,6
M_e	-	1,1	1,1	1,1
ω	-	30.3	30.3	30.3
ω_d	-	1	1	1
ξ	-	8,5	8,5	8,5
ξ_d	-	0.3	0.3	0.3
OCR	-	1,25	1,3	1,3
e_0	-	2,0	2,0	2,0
α_0	-	0,636	0,636	0,636
χ_0	-	8,0	8,0	8,0
τ	-	1,0	1,0	1,0
μ^*	-	0,00125	0,00125	0,00125
K_0^{NC}	-	0,368	0,368	0,368
k_x	m/day	0,0000864	0,0000864	0,00006912
k_y	m/day	0,0000864	0,0000864	0,00006912
E_{oed}^{ref}	kN/m^2	30000	30000	30000
c_{ref}	kN/m^2	3,0	3,0	3,0
$\varphi^{'}(phi)$	°	39,2	39,2	39,2
$\Psi\ (psi)$	°	0,0	0,0	0,0
$K_{0,x}$	-	0,6	0,6	0,6

B1 – Anisotropy and destructuration dependency for embankment

CHALMERS, *Civil and Environmental Engineering*, Master's Thesis BOMX02-16-103
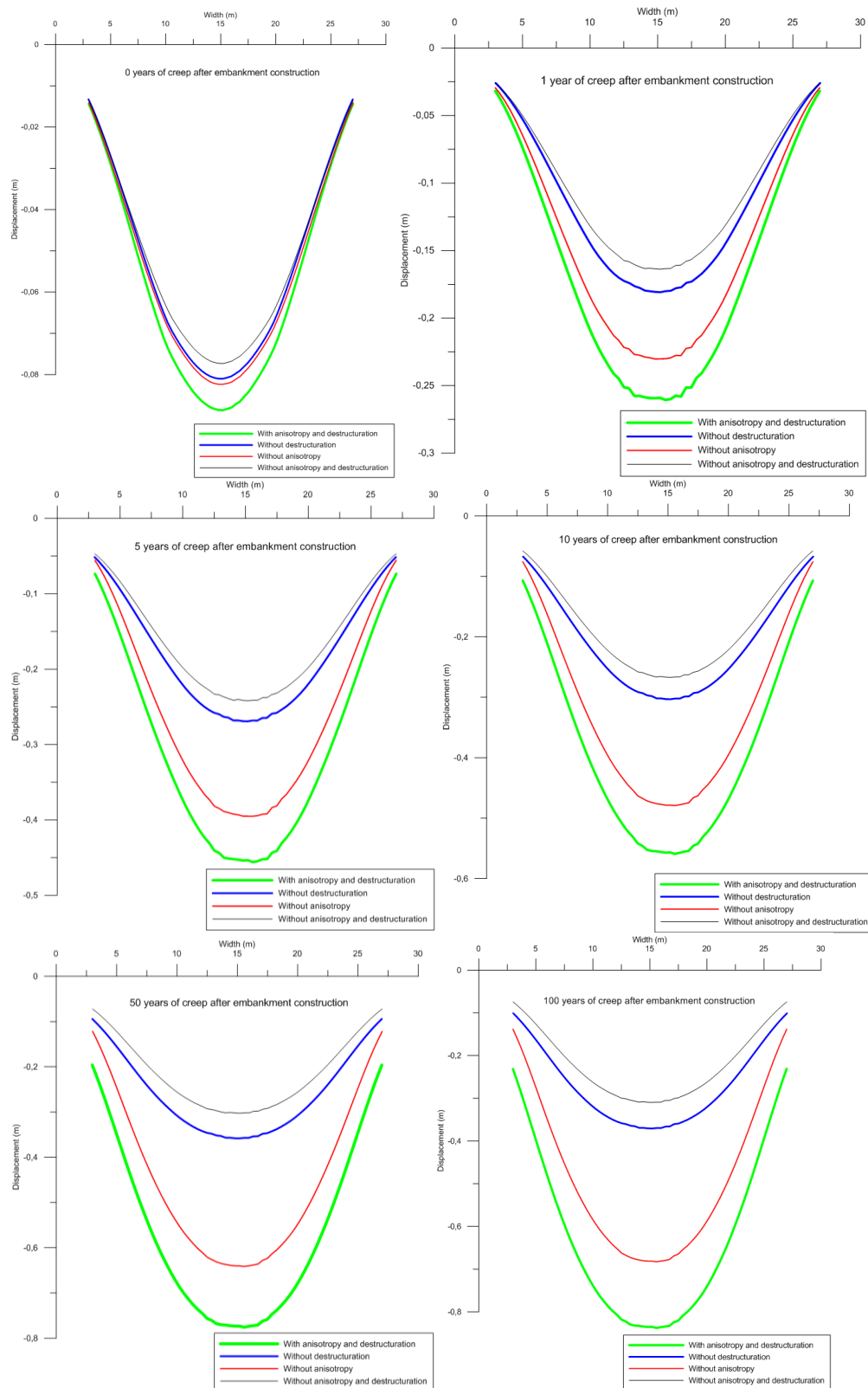
B2 – Anisotropy and destructuration dependency for excavation
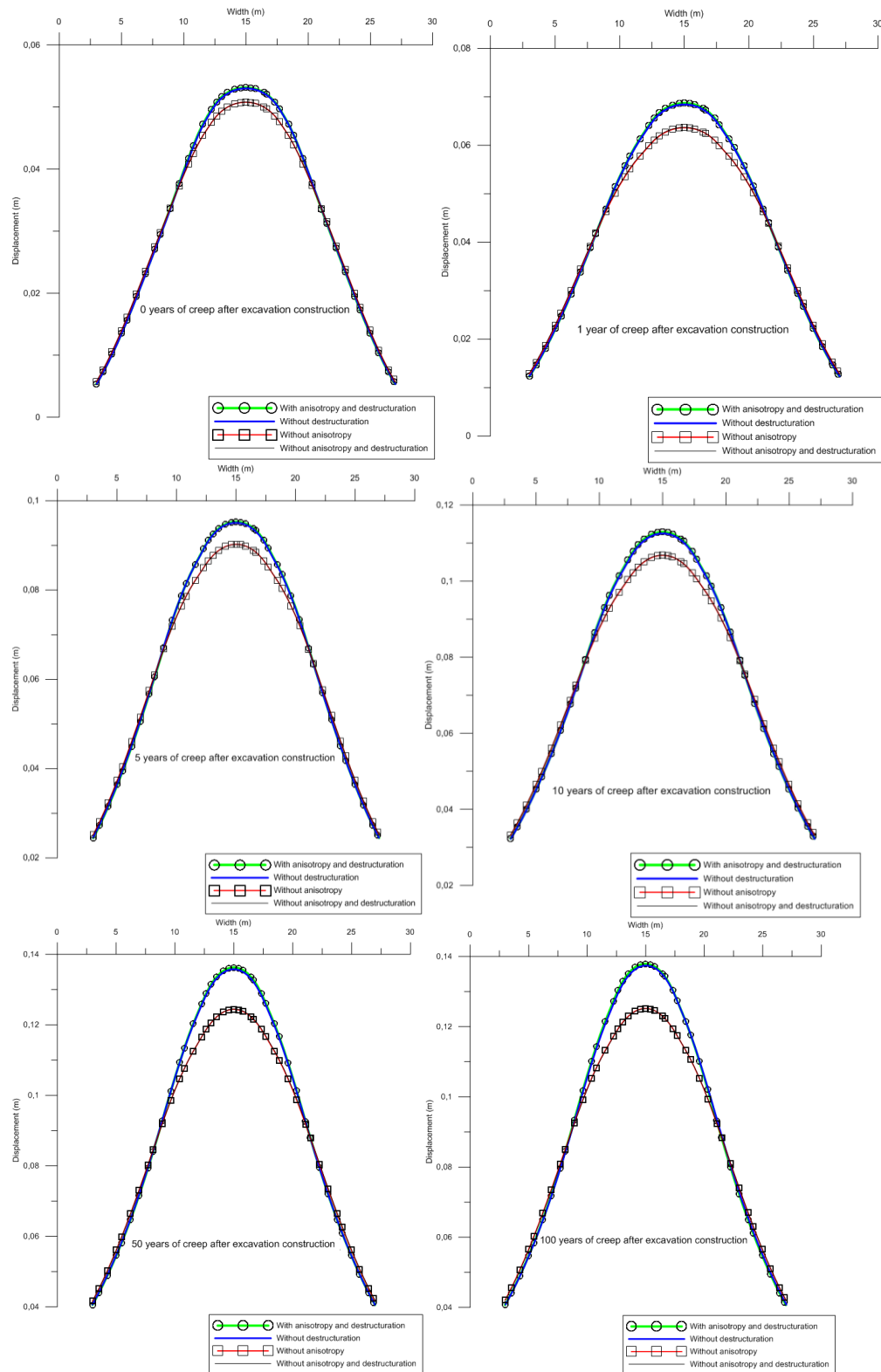
C1 – Active drained and undrained shear strength

CHALMERS, *Civil and Environmental Engineering*, Master's Thesis BOMX02-16-103
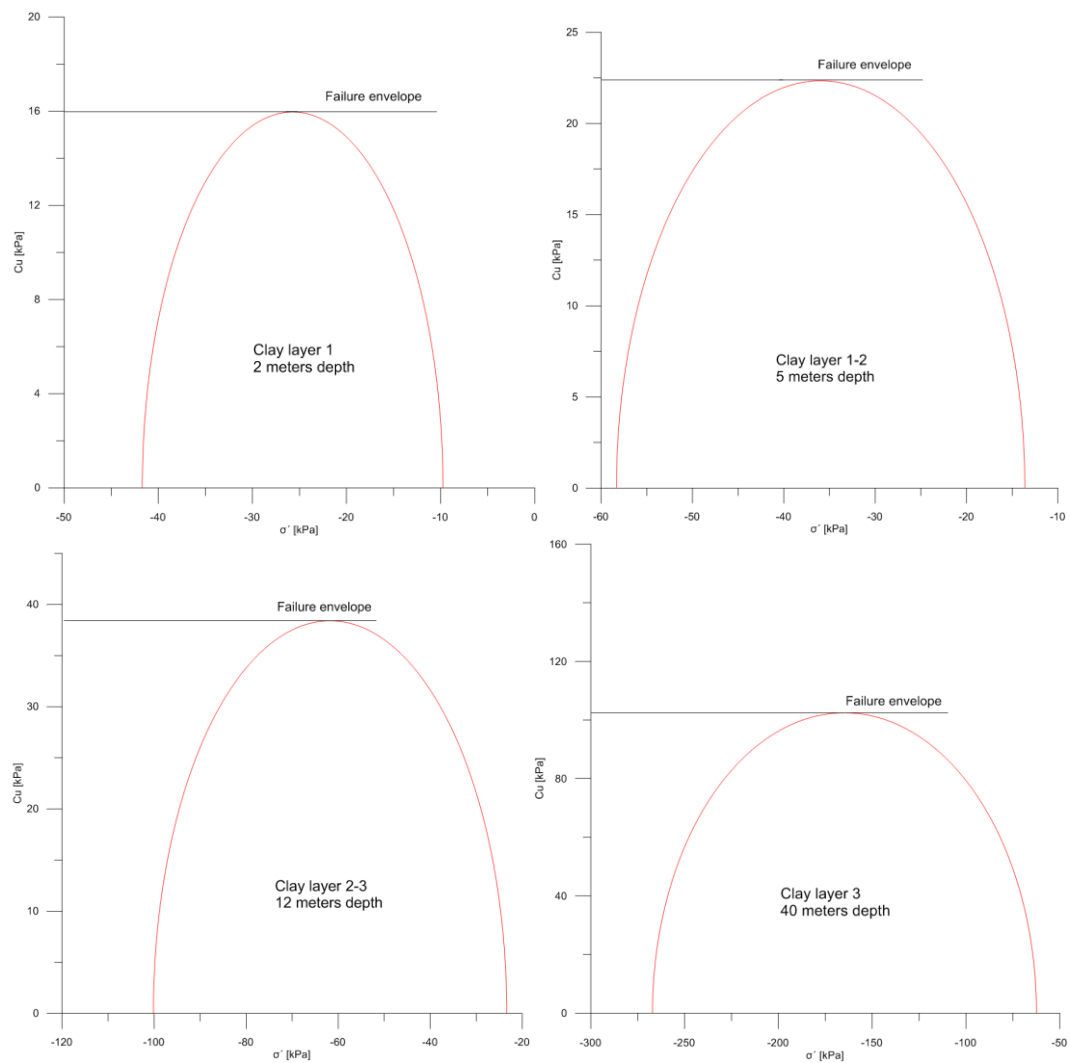
C2 – Passive drained and undrained shear strength